

In Amide Solvents:
A True Account of Multiple Metals for Catalysis and Their Consequences

by
Amanda M. Spiewak

A Dissertation Submitted in Partial Fulfillment of the
Requirements for the Degree of

Doctor of Philosophy
(Chemistry)

at the
UNIVERSITY OF WISCONSIN-MADISON

2020

Date of final oral examination: 7/17/2020

The dissertation is approved by the following members of the Final Oral Committee:

Daniel J. Weix, Professor, Chemistry
Tehshik P. Yoon, Professor, Chemistry
John F. Berry, Professor, Chemistry
Shannon S. Stahl, Professor, Chemistry

Dedication

I dedicate this work to my family, who have helped and supported me through this adventure in a way no one else could. You have all been and continue to be wonderful friends, confidants, advocates, and mentors to me.

I further dedicate this work to future generations entering the field of Chemistry as well as other STEM fields.

May you find a world worthy of your passion, dedication, and talent.

If you don't, help us build it.

Biographical Sketch

The author was born on February 27th, 1993 in Bethpage, New York and relocated to Charlton, Massachusetts. She attended the University of New Haven for her undergraduate studies. While there she conducted research on the characterization of heavy metal uptake by the *Phytolacca Americana*, and its potential for use for phytoremediation under the supervision of Professor Eddie Luzik. During the summer of 2013 she conducted a life cycle assessment of all of the chemistry laboratories offered through the University of New Haven under the supervision of Professor Can B. Aktas.

After graduating with two Bachelor's of Science degrees in Chemistry and Forensic Science in 2015, she joined the lab of Professor Daniel J. Weix at the University of Rochester. Her research focused on the development of a method for C-H arylation of naphthols via Ruthenium, the utilization of *N*-Hydroxyphthalimide esters and other activated redox active alkyl-forming reagents for use in cross electrophile coupling reactions, and the synthesis and mechanistic study of various metals for C-H activation and cross electrophile coupling. She received a Master's of Science from the University of Rochester in 2017. She was awarded the W.D. Walters Teaching Award from the Department of Chemistry in 2016.

In 2017, the author relocated with Professor Daniel J. Weix to the University of Wisconsin-Madison, where she joined the Science is Fun public engagement group under the supervision of Bassam Z. Shakhashiri in 2018 and was awarded College of Letters and Science Teaching Fellowship in 2019. After graduation, the author will be joining the

department of Chemistry & Biochemistry at the University of Wisconsin- La Crosse as an Associate Lecturer.

The following publications were a result of work conducted during doctoral study:

1. Huihui, K. M. M.; Caputo, J. A.; Melchor, Z.; Olivares, A. M.; Spiewak, A. M.; Johnson, K. A.; DiBenedetto, T. A.; Kim, S.; Ackerman, L. K. G.; Weix, D. J. “Decarboxylative Cross-Electrophile Coupling of *N*-Hydroxyphthalimide Esters with Aryl Iodides” *J. Am. Chem. Soc.* 2016, *138* (15), 5016-5019.
2. Spiewak, A. M.; Weix, D. J., “Ruthenium-Catalyzed C-H Arylation of 1-Naphthol with Aryl and Heteroaryl Halides” *J. Org. Chem.* 2019, *84*, 15642-15647.

Abstract

In this thesis,

Chapter 1 seeks to provide a description of cross electrophile coupling and the topic of metal-catalyzed reactions for the general public.

Chapter 2 describes the development of improved arylation conditions for the ruthenium-catalyzed C-H arylation of 1-naphthol with various aryl and heteroaryl halides. The application of these conditions, substrate scope, and limitations are also discussed.

Chapter 3 describes the development of nickel-catalyzed cross electrophile coupling of aryl halides and redox active esters and ethers.

Contributors and Funding Sources

This work was supervised by a dissertation committee consisting of Professors Daniel J. Weix (advisor), Tehshik P. Yoon, John F. Berry, and Shannon S. Stahl, of the Department of Chemistry. The author performed all experimental procedures in this dissertation unless specified below:

Chapter 3:

Work in this chapter was the product of the original research idea of the author and all experiments were carried out collaboratively with the author's undergraduate researcher, Polpum (Paul) Onnuch.

All the work included in this thesis was supported by the University of Rochester, the University of Wisconsin-Madison, and the National Institutes of Health.

Contents

Biographical Sketch	ii
Abstract	v
Contributors and Funding Sources.....	vi
List of Tables	x
List of Figures	xi
List of Symbols and Abbreviations.....	xiii
Chapter 1: Metal-Catalyzed Cross Electrophile Coupling.....	1
Chapter 2: Ruthenium-Catalyzed C-H Arylation of 1-Naphthols.....	16
2.1. Abstract	16
2.2. Introduction.....	16
2.3. Results and Discussion	18
2.3.1. Ancillary Ligand Screen	19
2.3.2. Dual Base System	20
2.3.3. Final Optimized Conditions	24
2.3.4. Evaluation of Substrate Scope	26
2.4. Conclusion	28
2.5. Experimental.....	29
2.5.1. Materials	29
2.5.2. General Methods	29

2.5.3. General Reaction Procedures	30
2.5.4. Product Characterization.....	32
References.....	40
Chapter 3: Nickel-Catalyzed Cross Electrophile Coupling of Aryl Halides and Redox Active Esters and Ethers	44
3.1. Abstract.....	44
3.2. Introduction.....	45
3.3. Results and Discussion	51
3.3.1. Initial Reaction Conditions	51
3.3.2. Trends with Ligands.....	53
3.3.3. Reaction Concentration Effects	57
3.3.4. Requirement of Acceptor/Donor Pair	58
3.3.5. Light Requirements.....	59
3.3.6. Optimizing for Ratio of Substrates	61
3.3.7. Potential Substrates.....	63
3.4. Conclusion	66
3.5. Experimental.....	68
3.5.1. Materials	68
3.5.2. General Methods.....	68
3.5.3. General Reaction Procedures	70
3.5.4. Product Characterization.....	73

List of Tables

Table 2.1 Abbreviated Ligand Screen for Aryl Iodides and Aryl Bromides	20
Table 2.2 Optimization of Base System for Aryl Iodides and Aryl Bromides	22
Table 2.3 Investigation of KOAc Loading Required.....	23
Table 2.4 Optimized Conditions for the Arylation of 1-Naphthol.....	25
Table 2.5 Aryl Iodides Under Conditions A Versus B	26
Table 3.1 Initial Investigation of NAP Ether Activation	52
Table 3.2 Initial Ligand Screen.....	54
Table 3.3 PyBCam Ligand Family Screen	56
Table 3.4 Concentration Investigation	58
Table 3.5 Determination of the Requirement of Hantzsch Ester	59
Table 3.6 Ascertaining the Necessity of Light on Reactivity.....	61
Table 3.7 Optimization of Substrate Ratio	62

List of Figures

Figure 1.1	3
Figure 1.2	4
Figure 1.3	5
Figure 1.4	6
Figure 1.5	7
Figure 1.6	8
Figure 1.7	9
Figure 1.8	11
Figure 1.9	12
Figure 1.10	13
Figure 1.11	14
Figure 2.1 Miura's Original Pd-catalyzed Arylation of 1-Naphthol.....	17
Figure 2.2 Conditions Developed for Similar Ru-catalyzed Arylation Reactions.....	18
Figure 2.3 Intermolecular C–H Arylation of 1-Naphthol with (Hetero)aromatic Halides ^a	27
Figure 2.4 Large Scale Arylation of 1-Naphthol	28
Figure 3.1 Methods for Conversion of Alkanoic Acids to Alkyl Radicals	47
Figure 3.2 Stoichiometric Reaction of Ni(II) Species and NAP Ether	53
Figure 3.3 Initial Catalytic Reaction Conditions	53
Figure 3.4 Initial Ligand Screen Product Distribution.....	55
Figure 3.5 PyBCam Ligand Family Product Distribution	57

Figure 3.6 Product Distribution at Various Substrate Ratios.....	63
Figure 3.7 Potentially Suitable N-Alkoxyphthalimide Ether Substrates	64
Figure 3.8 Initial Aryl Iodide Survey.....	64
Figure 3.9 Potential Ring-opening Substrates Under Current Reaction Conditions	65
Figure 3.10 Potential Ring-expansion with NAP Ether and Bromoallyl Silanes	66

List of Symbols and Abbreviations

- : minus, negative, or hyphen

% : percent

/ : per

: : ratio or colon

~ : about or approximately

° : degree(s)

+ : plus or positive

< : less than

> : greater than

× : multiplication, times, or by

°C : degrees Celsius

μm : micrometer(s)

¹³C : carbon-13

¹³C{¹H} : proton-decoupled carbon-13

¹⁹F : fluorine-19

¹⁹F{¹H} : proton-decoupled fluorine-19

¹H : proton

aq : aqueous

Ar : aryl

ASAP : atmospheric solids analysis probe

bathophen : bathophenanthroline (4, 7-diphenyl-1, 10-phenanthroline)

bpy : bipyridine

br : broad

Br : bromide

C : carbon or Celsius

C(sp²) : sp² hybridized carbon center

C(sp³) : sp³ hybridized carbon center

CD₂Cl₂ : deuterated dichloromethane

CDCl₃ : chloroform-*d*

Cl : chloride

cm : centimeter(s)

CMD : concerted metalation–deprotonation

CN : cyano, nitrile

cod : 1,8-cyclooctadiene

Cs₂CO₃ : cesium carbonate

CsOAc : cesium acetate

d : doublet

D₂O : deuterium oxide

DMA : *N,N*-dimethylacetamid

dme : dimethoxyethane

dppBz : 1,2-bis(diphenylphosphino)benzene

dppe : 1,2-bis(diphenylphosphino)ethane

dtbbpy : 4,4'-di-*tert*-butyl-2,2'-dipyridyl

equiv : equivalent(s)

ESI : electrospray ionization

Et₂O : diethyl ether

EtOAc : ethyl acetate

EtOH : ethanol

FID : flame ionization detector

g : grams(s)

GC : gas chromatography

GCMS : gas chromatography-mass spectrometry

h : hour(s)

H : hydrogen

HCl : hydrochloric acid

HRMS : high-resolution mass spectrometry

Hz : Hertz

I : iodide

I₂ : iodine

J : coupling constant

K₂CO₃ : potassium carbonate

KOAc : potassium acetate

L : ligand

LED : light emitting diode

LiBr : lithium bromide

LiCl : lithium chloride

M : metal or molar

m : multiplet

m/z : mass-to-charge ratio

MeO : methoxy

MeOH : methanol

mg : milligram(s)

MgSO₄ : magnesium sulfate

MHz :mega Hertz

min : minute(s)

mL : milliliter

mm : millimeter(s)

mmol : millimole

Mp : melting point

MS : mass spectrometry

N : substituted or positioned on nitrogen

N₂ : nitrogen

Na₂SO₄ : sodium sulfate

NaCl : sodium chloride

NaHCO₃ : sodium bicarbonate

NaHSO₄ : sodium bisulfate

NAP : *N*-alkoxyphthalimide

NHP : *N*-hydroxyphthalimide

Ni : nickel

nm : nanometer(s)

NMP : 1-Methyl-2-pyrrolidinone

NMR : nuclear magnetic resonance

o : ortho

O : oxygen

OAc : acetate

OH : hydroxyl

OLED : organic light emitting diode

p : para

PCy₃ : tri-cyclohexyl phosphine

Pd : palladium

phen : phenanthroline

PPh₃ : triphenylphosphine

ppm : parts per million

psi : pounds per square inch

PTFE : polytetrafluoroethylene

PyBCam : pyridine-2,6-bis(carboxamidine)

q : quartet

rpm : revolutions per minute

rt : room temperature

Ru : ruthenium

s : singlet

SET : single electron transfer

T : temperature

t : triplet

*t*Bu : *tert*-butyl

terpy : terpyridine

THF : tetrahydrofuran

TMS : tetramethylsilane

UV : ultraviolet

UV-vis : ultraviolet-visible

vs : versus

X : halide or pseudohalide

XCR : cross-coupling reaction

XEC : cross-electrophile coupling

β : beta

δ : delta, chemical shift

μ L : microliter(s)

Chapter 1: Metal-Catalyzed Cross Electrophile Coupling

As the first chapter of my doctoral thesis, I am thankful to have had the opportunity to explain my research to a broad, non-scientific audience. Through the sponsorship and support of the Wisconsin Initiative for Science Literacy at the University of Wisconsin- Madison, I have been able to create the following chapter to illuminate the type of work I have been engaged in during my graduate studies in chemistry. Since all scientific research is conducted in the service of obtaining knowledge to better the human condition and advance society, it is imperative that findings are communicated broadly to all members of society. Therefore, I believe that it is the duty of scientists to communicate scientific research that has been done in the service of all in a way that is accessible and understandable by everyone. To this end, I have formulated the following description of the type of research conducted in my group at UW-Madison, as well as some of my recent results and findings.

I have always had fond memories of playing with LEGO blocks alongside my older brother when I was growing up. As I look back on these times, I think that I, as many others before me, enjoyed the ability to create anything I could imagine from these simple blocks. I spent hours simply putting various blocks together and taking pieces away when I found I no longer needed them or exchanging a red brick for a green one because it looked nicer to me. Now, as I write what will become the first chapter of my thesis for my chemistry doctoral degree, I reflect on how most of my work in this field reminds me of the days when I would build new creations with my LEGOs.

I am a synthetic chemist by trade, which means I'm particularly good at finding new ways to make molecules. A molecule is the simplest unit of a chemical compound that can exist, consisting of two or more atoms held together by chemical bonds. For instance, water is a chemical

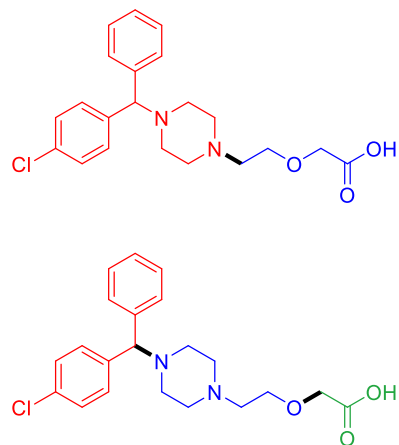
compound made up of molecules that are each one oxygen atom bonded to two hydrogen atoms which gives it the molecular formula of H_2O . Where I once used blocks to create buildings in my make-believe towns growing up, I now find new ways to use chemicals to construct complex molecules that could be of use to our society. The method that I use to make these molecules is called cross electrophile coupling (XEC), and I hope that you will follow me on an intellectual adventure and allow me to share with you how this particular type of chemistry works.

First and foremost, I'd like to talk about why many chemists (myself included) have been trying to think of creative new ways to put together molecules for many decades now. What we seek as a community is the ability to access what LEGOs allow: the capacity to build anything we can think up. For synthetic chemists, this means the capability to access any molecule they believe would help our society- be it to make new materials for better aircrafts, high-performance batteries for electric vehicles, or even the next anticancer drug. We call these sorts of molecules of interest "target molecules." Much like the "target" of making a LEGO house could be achieved by different formations of building blocks, we achieve the synthesis of a target molecule by piecing together smaller molecular blocks, which we even refer to at times as "building blocks" (Figure 1.1). This is what the community seeks: new ways to make a target molecule that are faster, more reliable, or cheaper than previous methods. We are also always on the lookout for ways to make target molecules that scientists haven't been able to "piece together" just yet, so every method we add to our community's toolkit helps to reach targets we may not have been able to in the past.



Figure 1.1

Two ways to build the same LEGO house (left), and two ways that you can make the molecule Cetirizine, commonly called Zyrtec, from smaller molecular fragments (right).



As I mentioned before, my group specializes in a specific method of making target molecules. We are helping to expand one of many different categories of synthetic chemistry called cross electrophile coupling, and we have a few reasons to believe that this sort of chemistry will be immensely helpful when it comes to expanding the amount of target molecules we can make that synthetic chemists haven't been able to access before. But first, I want to take time to explain how we piece our molecules together and what makes XEC different from other methods, namely traditional cross coupling reactions.

All cross-coupling reactions (XCRs) seek to make a target molecule by forming connections we call bonds between two or more smaller molecular pieces. This can be thought of like LEGOs trying to fill an area on a base plate (we will outline it and call it our target molecule in Figure 1.2) by finding two LEGOs that can fit together to fill the available space. Metal-catalyzed XCRs use a metal to bind and put the target molecule pieces together. This metal is called a catalyst in these reactions because it helps to speed up the chemical reaction but is not consumed by the reaction. This means we can use just a small amount of the catalyst in order to make our “target molecule,” just as you can put many pairs of LEGOs together even though you are one person. Much like you select two LEGOs with your hands to place them in the outline of your “target molecule,” the metal catalyst will bond with one of each of the smaller molecules that make up the target molecule and eventually form the required bond between them. How does this metal know which piece is which though?

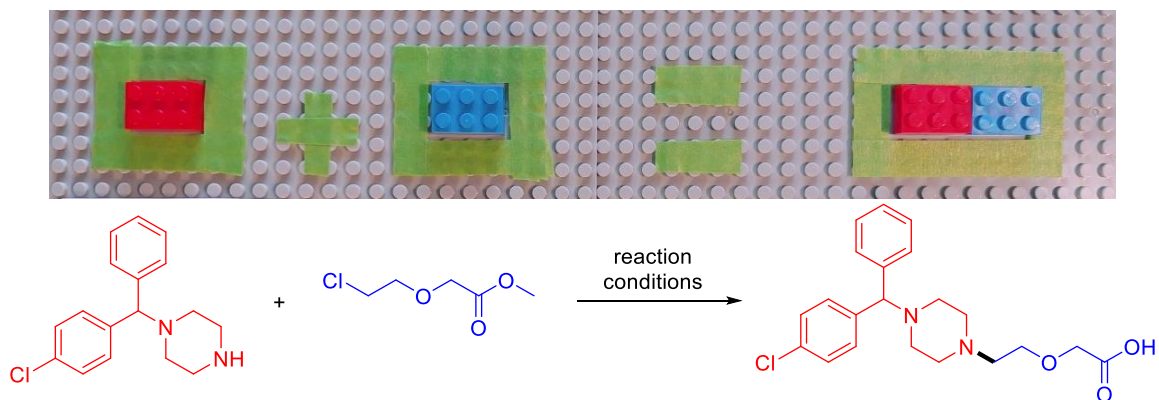


Figure 1.2

Two LEGOS (left side) are added together to form our “target molecule” (right side). This is akin to forming a bond to make our target molecule Cetirizine (Zyrtec) from two molecular fragments (shown below).

Just as you use your eyes to see the size and color of the LEGO you are using, and determine which two to place down to make your target molecule, the metal catalyst we choose

can also “look” at a set of molecular pieces and determine which ones it will put together. Catalysts achieve this ability to distinguish between the molecular fragments we call coupling partners by having a different affinity for various reactive groups on the fragments. In traditional XCRs, the coupling partners are distinguishable by the fact that one has a chemical species that can donate an electron (the universe's fundamental unit of negative charge) pair to form a bond with our catalyst (called a nucleophile) that reacts differently than the other partner, which will accept an

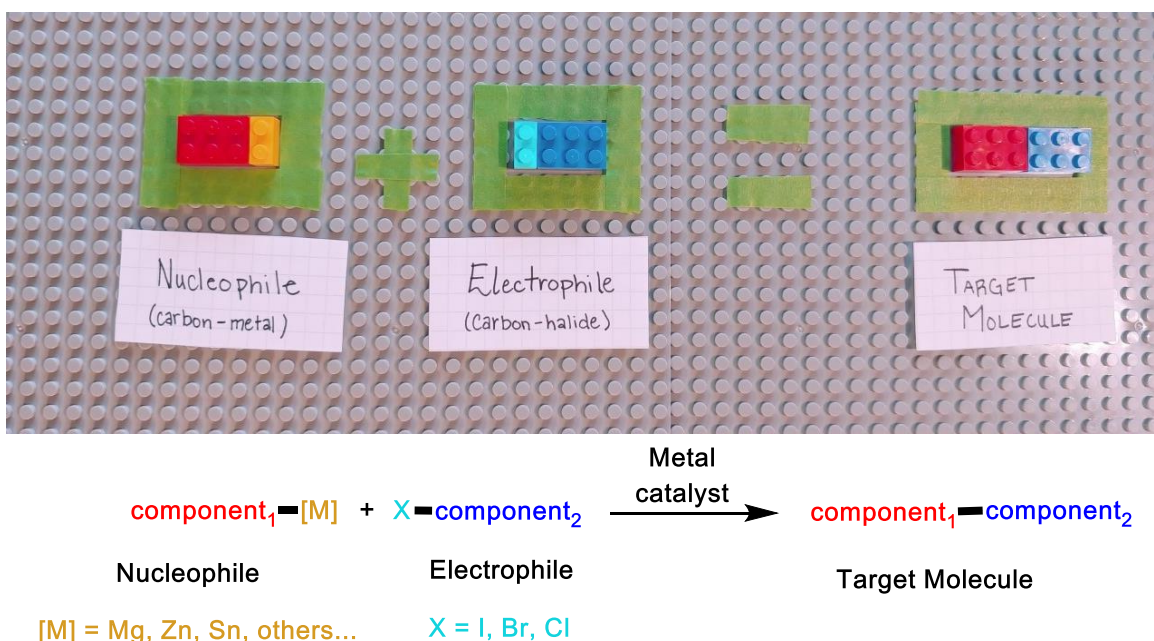


Figure 1.3

A target molecule made via traditional XCR, where we use a nucleophile (yellow LEGO representing the metal reagent that our carbon piece is bonded to) and an electrophile (light blue LEGO representing the halide that our carbon piece is bonded to). The same scheme is represented chemically below this image.

electron pair to form a bond with our catalyst (called an electrophile) (Figure 1.3). Nucleophiles tend to contain an electron rich carbon-metal bond, that is, a bond between a carbon atom and one atom of almost any element in the first 13 columns of the periodic table, as well as a few more (as shown in silver in Figure 1.4). Scientists have determined that these elements are metals based on bulk material properties they share, such as high electrical conductivity, luster, and malleability

(its ability to be chapped by force, such as being hit with a hammer to be flattened or bent).

Electrophiles on the other hand, contain electron deficient bonds, most of which are bonds between

1																	18
H																	He
3	4											5	6	7	8	9	10
Li	Be											B	C	N	O	F	Ne
11	12											13	14	15	16	17	18
Na	Mg											Al	Si	P	S	Cl	Ar
19	20	21	22	23	24	25	26	27	28	29	30	31	32	33	34	35	36
K	Ca	Sc	Ti	V	Cr	Mn	Fe	Co	Ni	Cu	Zn	Ga	Ge	As	Se	Br	Kr
37	38	39	40	41	42	43	44	45	46	47	48	49	50	51	52	53	54
Rb	Sr	Y	Zr	Nb	Mo	Tc	Ru	Rh	Pd	Ag	Cd	In	Sn	Sb	Te	I	Xe
55	56	57-71	72	73	74	75	76	77	78	79	80	81	82	83	84	85	86
Cs	Ba		Hf	Ta	W	Re	Os	Ir	Pt	Au	Hg	Tl	Pb	Bi	Po	At	Rn
87	88	89-103	104	105	106	107	108	109	110	111	112	113	114	115	116	117	118
Fr	Ra		Rf	Db	Sg	Bh	Hs	Mt	Ds	Rg	Cn	Nh	Fl	Mc	Lv	Ts	Og
57	58	59	60	61	62	63	64	65	66	67	68	69	70	71			
La	Ce	Pr	Nd	Pm	Sm	Eu	Gd	Tb	Dy	Ho	Er	Tm	Yb	Lu			
89	90	91	92	93	94	95	96	97	98	99	100	101	102	103			
Ac	Th	Pa	U	Np	Pu	Am	Cm	Bk	Cf	Es	Fm	Md	No	Lr			

Figure 1.4

A periodic table of the elements with all the metals highlighted in silver. Halogen elements are boxed in red. (figure source: <https://sciencenotes.org/list-metals/>)

carbon atoms and a halogen atom. Halogens are the elements in the 17th column of the periodic table (Figure 1.4), and as a group also share a distinct quality: they are one electron away from having a full outer shell of electrons. This property, from which the term halogen is derived (the name halogen means “salt producing”) causes these atoms to form ionic, or salt-like bonds with other atoms that are electron deficient due to the halogen accepting an electron from the atom to which it bonds in order to fill its outer shell of electrons (Figure 1.5).

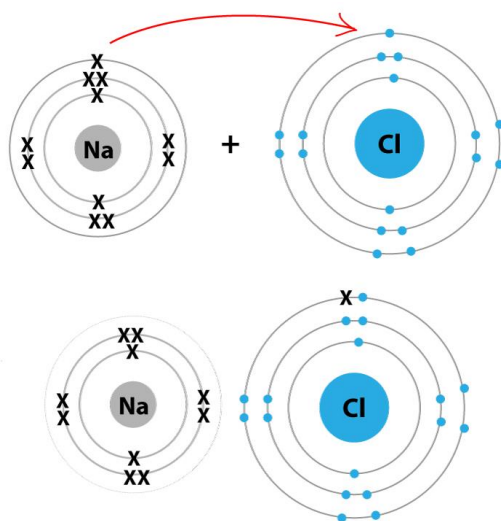


Figure 1.5

Here is a diagram of the chlorine atom, a single atom of the second earliest of the halogen elements. Its atomic number is 17, and thus it has 17 electrons (as well as 17 protons for an overall neutral or lack of charge). With 17 electrons (depicted by the blue dots) however, the chlorine atom has one unpaired electron in its outer shell (shells depicted by the circles). Accepting one electron from an atom of say, sodium (atomic number 11, capable of donating its unpaired electron, represented by the black X) will cause both atoms to be bound ionically, giving each atom a filled outer shell of electrons and making the ionic compound of table salt, NaCl. (figure source: <https://vivadifferences.com/covalent-vs-metallic-vs-ionic-bond-differences-and-examples/>)

The strength and reactivity of these two types of carbon bonds is different enough that our metal catalyst can react with one bond before the other. This idea is similar to thinking about what might happen if you were to hold two rubber bands of similar length but differing thicknesses between your hands and then pull on them in order to break them. It is likely that the thinner band would break first, since it isn't as tough as the thicker band, thus requiring less energy to snap. Similarly, certain bonds require less energy for different metals to break as well. This varies based on the identity of the metal catalyst, which allows chemists to choose metals that activate the bonds we want. Using some special catalysts helps my group to make some interesting new molecules through XEC (cross-electrophile coupling).

As the name suggests, XEC is a method in which the target molecule's bond is formed by piecing together two coupling partners that each contain a carbon-halide bond (two electrophiles) rather than making the bond from one electrophile and one nucleophile (Figure 1.6). This gives us

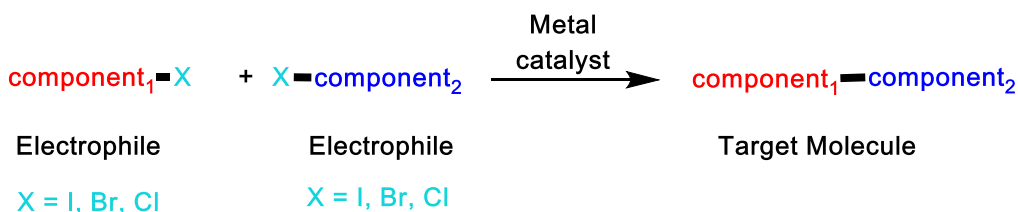
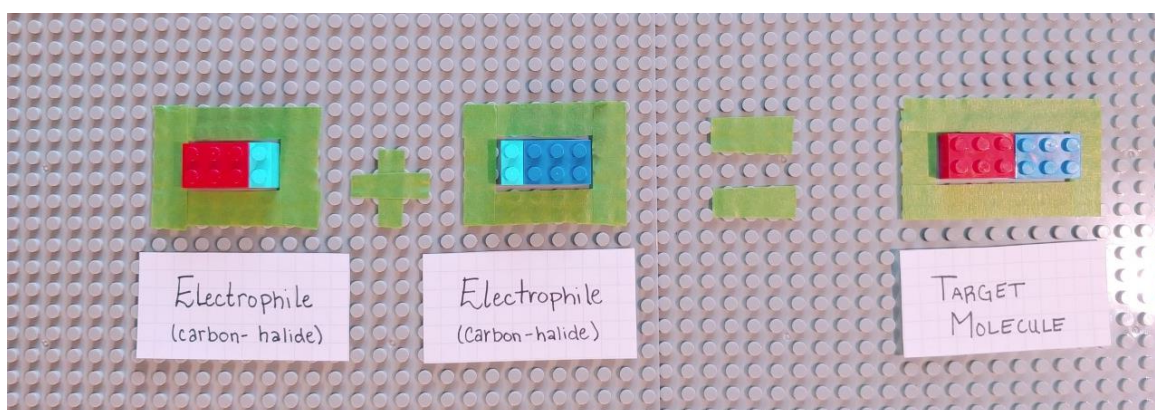


Figure 1.6

A target molecule made via XEC, where we use two electrophiles (light blue LEGO representing the halide that our carbon piece is bonded to) each bearing a fragment needed in our final molecule. The same scheme is represented chemically below this image.

access to over 300 times more coupling partners to make our bonds with when compared to nucleophiles that we would use in a standard XCR! That is to say, 99.7% of available molecular pieces for cross coupling are electrophiles, and only 0.3% are nucleophiles (Figure 1.7). Imagine how many more target molecules could be accessed if you can put two of these electrophiles together instead of always using 0.3% of the total pool of pieces to make up half of the molecule every time. This ability is what drives my group and many others to undertake the more difficult task of selecting a proper catalyst to accommodate the coupling of two electrophiles.



Figure 1.7

A LEGO representation of the availability of electrophiles versus nucleophiles for XCRs. This is 1000 LEGOs, so 997 represent electrophiles, and the three purple LEGOs at the bottom right represent the available nucleophiles.

The coupling of two pieces from the remaining 99.7% of the available pool requires extremely sensitive catalysts. This makes the main goal of my research (described in the following chapters) to find suitable reaction conditions so that the metal catalyst I use in my reaction can correctly choose one of the coupling partners first, even though they are similar in reactivity (Figure 1.8). By changing the identity of the catalyst as well as other additives present in my reactions (such as the solution in which the chemistry takes place), I work to achieve total (100%)

coupling of the two fragments I choose. Sometimes, the metal catalyst doesn't work as I hope it would and gives interesting but undesired coupling of the molecular fragments I'm working with. In these sorts of cases, the metal acts as you might if someone blindfolded you and asked you to put two LEGOs together to make a target molecule. Imagine trying to place two LEGOs on our target molecule outline, but you can only select from a pile containing all blue and red bricks, each brick the same dimensions. You may pick LEGOs that are different colors at times (these would represent our desired cross coupled product) or put two of the same colored LEGOs together since you cannot see (Figure 1.8).

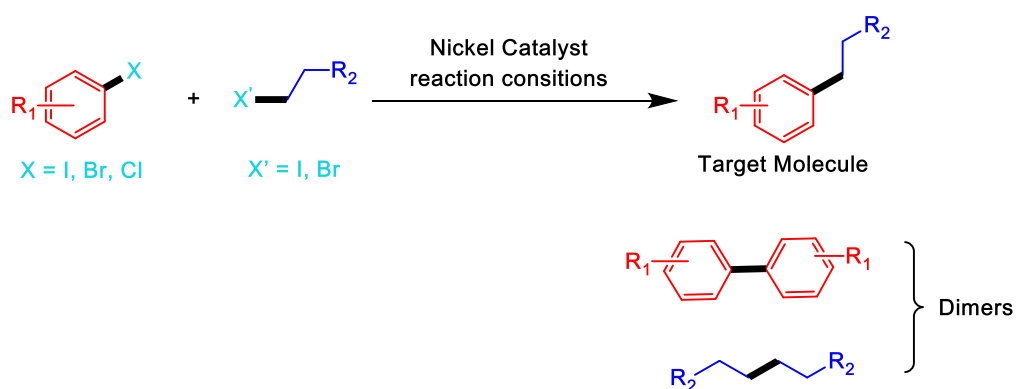
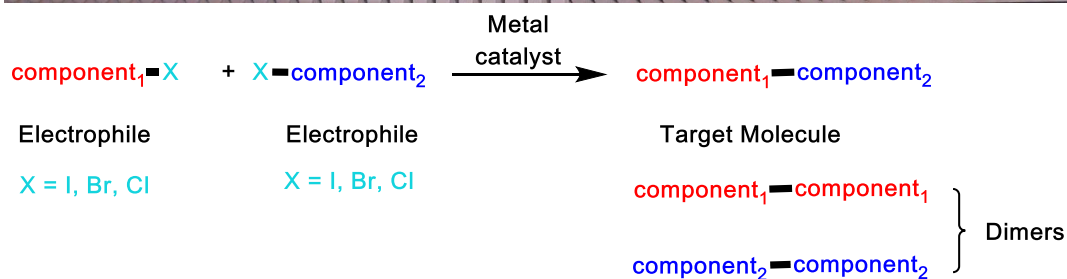
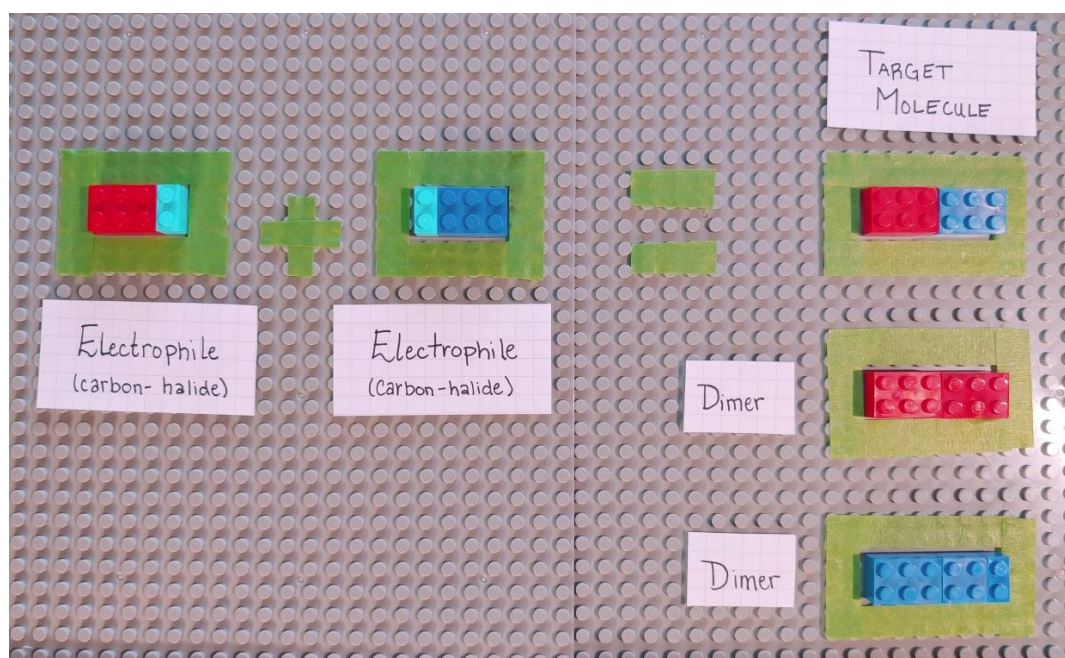


Figure 1.8

At top, a LEGO representation of a XEC, as well as the unwanted dimer side products formed. At center, the same scheme is represented chemically. At bottom, a reaction conducted in my research group showing the color-coded electrophiles, target molecule, and similar dimers formed.

In the case of XEC, we refer to the coupling between two of the same coupling partners as a dimer (two of the same pieces). To figure out how to make reactions with side products like dimers start to give target molecules instead, we need to understand how these dimers are forming. Below is one of the reactions I have recently worked on (Figure 1.9) that started out with a lot of unwanted dimers. This reaction is the Ni-catalyzed XEC between iodobenzene (that's an example of an electrophile where a carbon is bonded to an iodide, in red) and an *N*-alkoxyphthalimide ether (this molecule acts as an electrophile as well, in blue) to make our target molecule in red and blue, as well as two dimers (the red-red coming from two iodobenzene molecules coupling, and the blue-blue from two *N*-alkoxyphthalimide ether molecules).

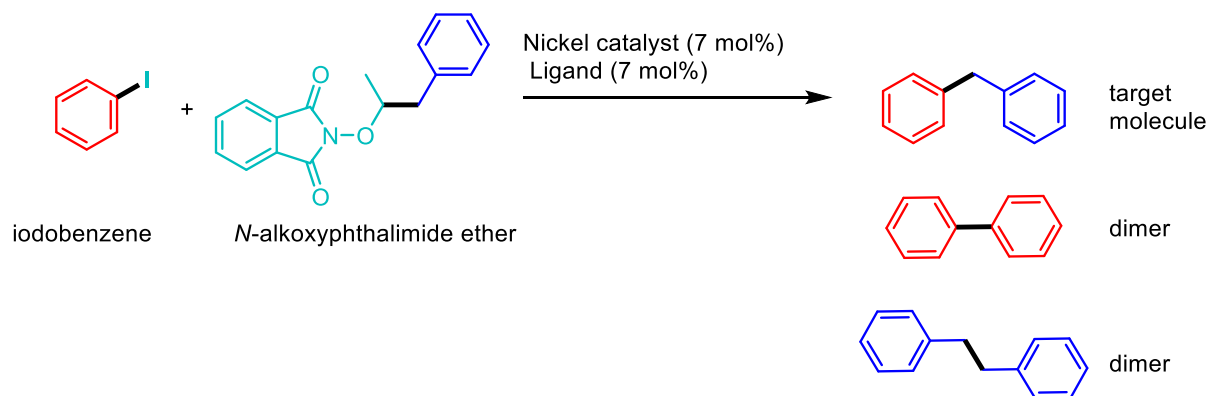


Figure 1.9

A XEC that I have spent time during my work at UW-Madison to perfect, such that it gives mostly the first product (target molecule) shown.

At first, this reaction gave a lot of the dimer made from two of the *N*-alkoxyphthalimide ether molecules (that molecule, labeled as dimer at the bottom of figure 1.9 in blue is called bibenzyl). To attempt to make our catalyst better at distinguishing between the two coupling partners in order to get more target molecule rather than this dimer, we looked into different ligands. Ligands are molecules that can attach themselves (by forming bonds) to our nickel catalyst

and change how it interacts with our coupling partners. In figure 1.10, you can see the first ligand screen we ran, as well as the structures of some of these ligands. I've also included a bar graph to

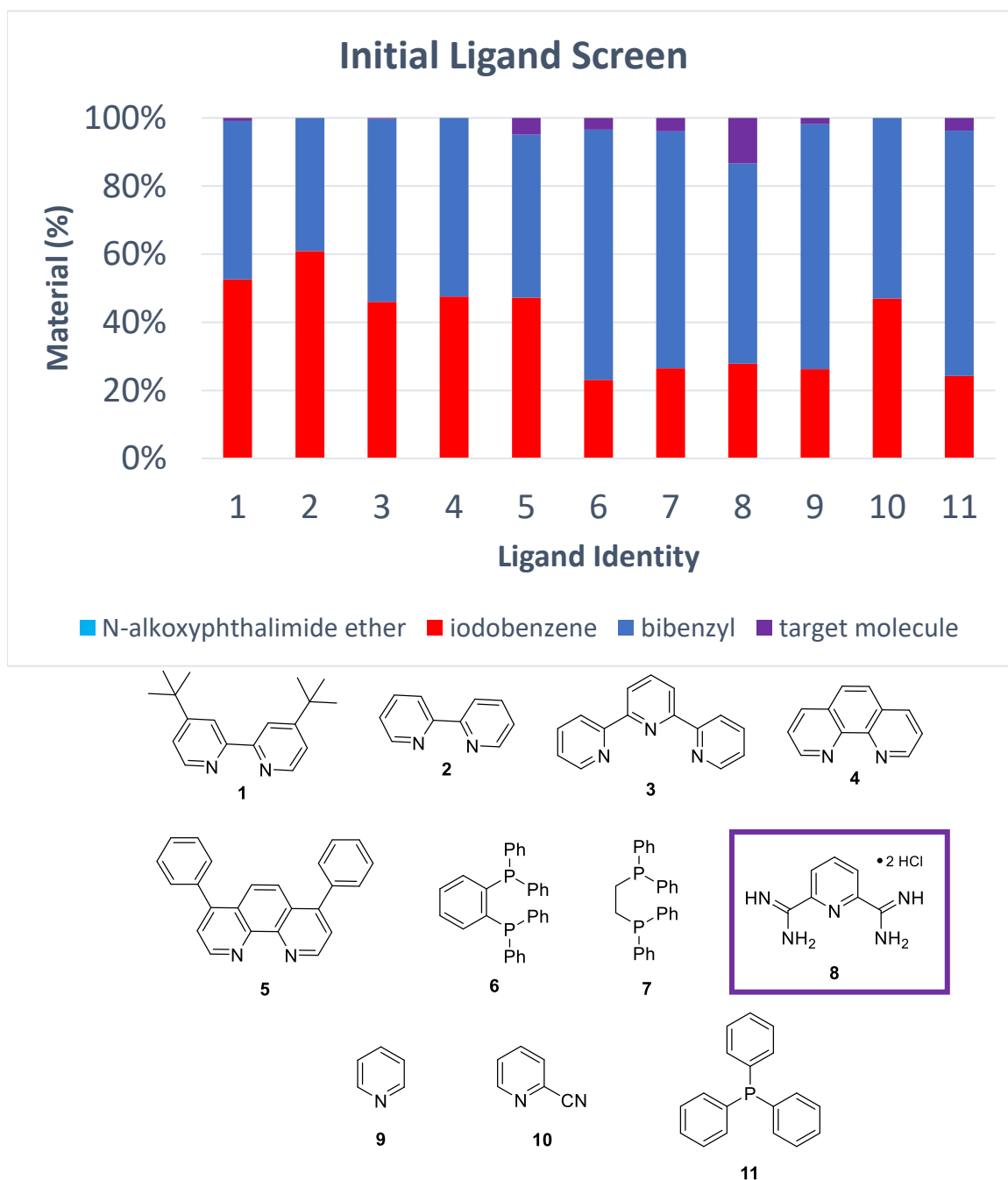


Figure 1.10

A graph of the distribution of molecules made using different ligands on our nickel catalyst. The boxed ligand, 8, gives the highest percentage of the target molecule, 23%.

show how much target molecule is made versus bibenzyl, and if we have coupling partners left after 17 hours of running our reaction (this would be like just having leftover LEGOs that we didn't use to make anything). Since ligand 8 gave the highest percentage of our target molecule (in purple) but still had a lot of bibenzyl (in blue, one of the dimers we didn't want), we took a look at ligands similar to it (shown in Figure 1.11). We were elated to find a version of ligand 8 (labeled

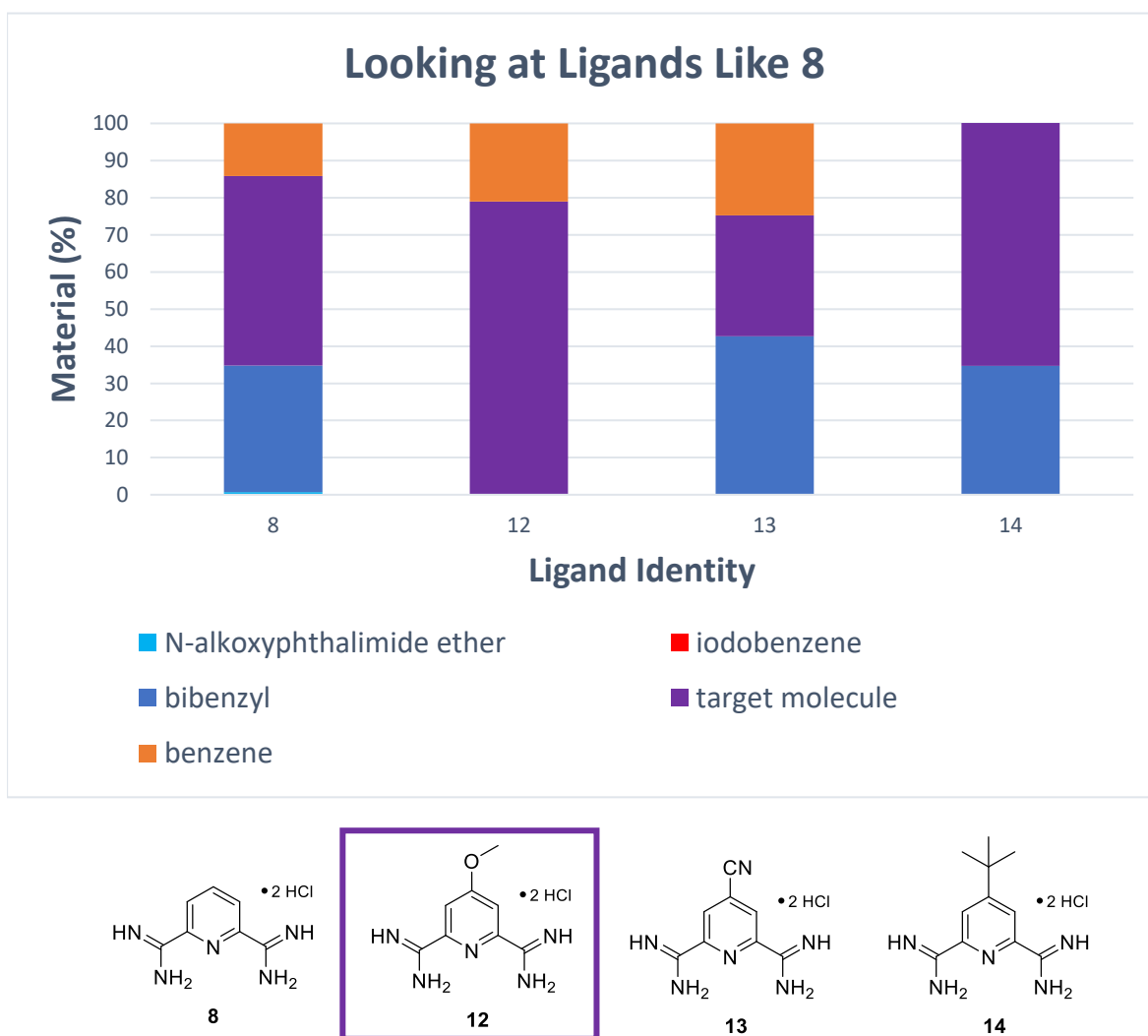


Figure 1.11

A graph of the distribution of molecules made using different ligand on our nickel catalyst. The boxed ligand, 12, gives the highest percentage of the target molecule, 78% and gives no dimers.

12 and boxed) that actually gives the target molecule in 78% yield and without any dimers as side products. Instead, we ended up getting just a small amount (22%) of the original iodobenzene returned without the iodide attached. This happens when the nickel catalyst can break the carbon-halogen bond in order to pick up this coupling partner by bonding to it, but then becomes unbound from the carbon portion. This was still a great finding, and we have been looking into other conditions for our reaction to give only target molecule and reduce this new side product.

Some of my research recently has also been aimed at understanding where the undesired side products in my group's chemistry come from. We hope that understanding this will allow us to find new ways to avoid these side products and make more of our target molecule. Once XEC can be understood in this way, synthetic chemists should have more of the tools they need to make anything they can think up. It is my hope that this expanded understanding will allow my community to benefit from lots of great new molecules!

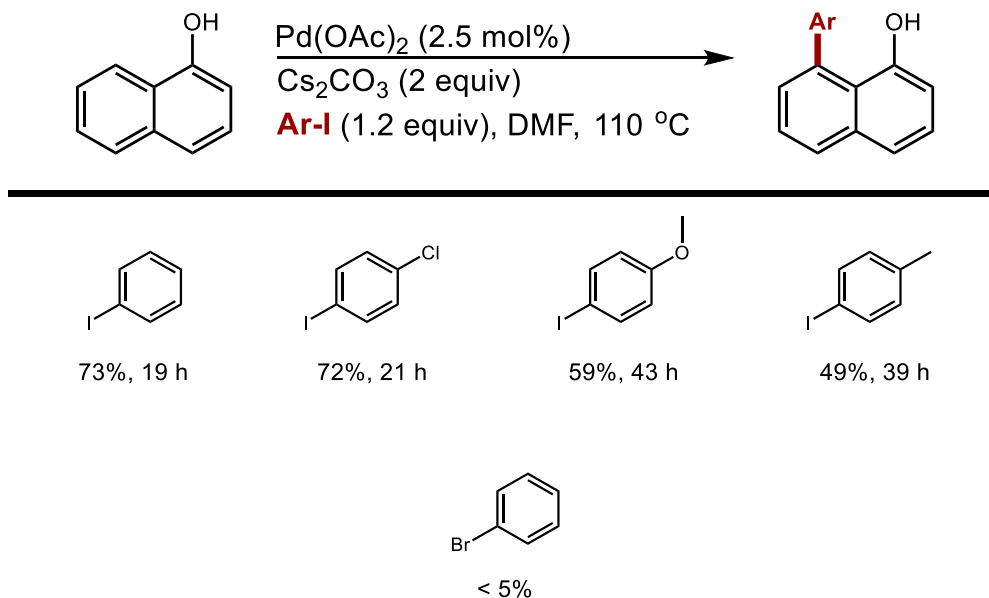
Chapter 2: Ruthenium-Catalyzed C-H Arylation of 1-Naphthols

2.1. Abstract

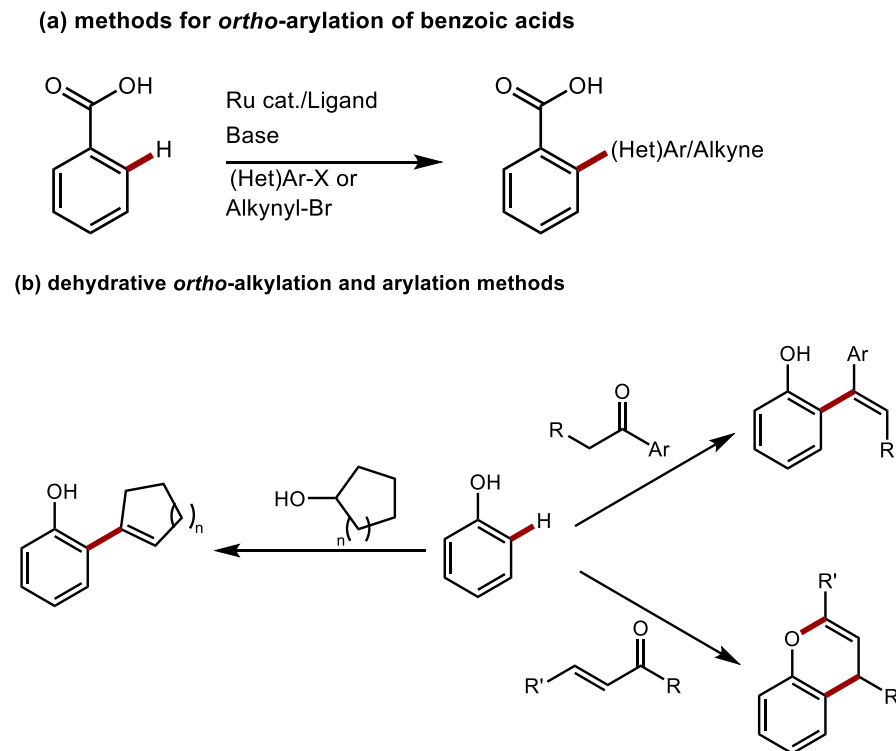
Transition metal catalyzed C-H arylation can streamline synthesis by avoiding the need for prefunctionalization, but selective reaction with one C-H bond out of many can be challenging.¹⁻¹⁰ Directed C-H arylation has proven to be one of the most robust approaches to solving this problem.⁴⁻¹⁰ **Error! Bookmark not defined.** Methods that rely upon innate functional groups as directing groups rather than the introduction and removal of specialized groups can be especially efficient, albeit often at the expense of more narrow applicability.¹¹⁻¹⁷ These methods can nonetheless open up new chemical space for exploration. In particular, 8-aryl-1-naphthol derivatives are being interrogated for use in organic light emitting diode (OLED) applications.¹⁸ In addition, easy access to these 8-arylated naphthols simplified access to fluoranthenes.^{19,20}

2.2. Introduction

The development of a method to access 8-aryl-1-naphthol derivatives from 1-naphthol by Miura (Figure 2.1)^{21,22} allowed for a variety of these motifs to be synthesized via a Pd-Catalyzed C-H arylation directed by the phenolic group of the naphthol. While this palladium-catalyzed C-H arylation procedure was a powerful advance, the method only provided high yields with aryl iodides and functional-group tolerance was limited: no examples with aniline functional groups or heteroaromatic halides were provided.²³ This is problematic because the more promising 8-aryl-1-naphthol dyes contain heteroaromatic or highly substituted aryl groups, requiring lengthy cross-coupling approaches involving protection/deprotection steps.¹⁸

Figure 2.1 Miura's Original Pd-catalyzed Arylation of 1-Naphthol

Ruthenium-catalyzed C-H arylation in some cases has been demonstrated to be superior to the analogous palladium-catalyzed methods.^{6,10,17} For example, our group, along with Gooßen, Ackermann, and Larossa, found that ruthenium catalysts are more tolerant of heteroaromatic halides and less reactive aryl halides in the *ortho*-arylation of benzoic acids (Scheme 2.2a).²⁴⁻²⁷ *peri*-Arylation with naphthols has not been reported, but *ortho*-alkylation of phenols and naphthols^{28,29} and *ortho*-arylation of 2-pyridyl-protected phenols has been reported (Scheme 2.2b).³⁰

Figure 2.2 Conditions Developed for Similar Ru-catalyzed Arylation Reactions

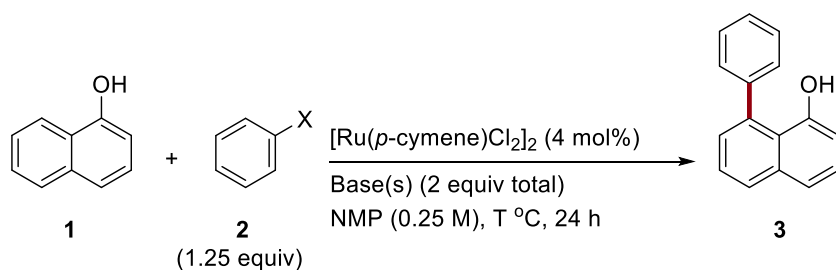
2.3. Results and Discussion

Starting with the previously optimized conditions for the ruthenium-catalyzed C-H arylation of benzoic acids found by Dr. Liangbin Huang in our lab²⁴, the arylation of 1-naphthol with iodobenzene was interrogated as a model substrate pair. We believed that utilizing ruthenium would allow for a more robust C-H arylation than had been achieved by Miura with palladium, as we had seen success with this catalyst when utilizing aryl-functionalities that generally gave poor yields in the analogous palladium-catalyzed carboxylic-acid directed chemistry. For this reaction, we anticipated that utilization of ruthenium in place of palladium would allow us access to less reactive aryl-halide bonds, such as aryl-bromide and chloride bonds, as well as impart the

functional group tolerance we desired for hetero-aryl groups. Three major findings during the reaction-screening process led to optimized reaction conditions requiring no ligand, a dual base system, and two complimentary sets of overall reaction conditions for different type of aryl substrates. These findings are discussed in detail below.

2.3.1. Ancillary Ligand Screen

Initially it was believed that the reaction conditions would need to include an ancillary ligand, as we had seen success in utilizing monodentate phosphine ligands (namely tri-cyclohexyl phosphine, PCy₃) in our ruthenium catalyzed C-H activation of aryl carboxylic acids. It appeared that the same ligand would be needed to facilitate productive reactivity in initial screenings using iodobenzene as the arylating reagent but did not appear to be the correct ligand when looking into conditions for bromobenzene. Thus, a more in-depth search for ligands suitable for the aryl bromide conditions was performed (some abbreviated results are in Table 2.1 entries 4 to 8), leading to phenanthroline (phen) to be considered the optimal ligand. When control reactions were run for both conditions (more prominently apparent in the case of the aryl bromide conditions (Table 2.1, entries 1 and 4)) neither system appeared to require an ancillary ligand to deliver the product in good yield. In fact, the yield of the aryl bromide derived product was increased by almost 20% when the ligand was omitted entirely (Table 2.1, entries 4 and 6). This information led to the omission of any additional ligand in our system.

Table 2.1 Abbreviated Ligand Screen for Aryl Iodides and Aryl Bromides

entry ^a	X	base(s) ^b	ligand ^c	T (°C)	yield ^d (%)
1	I	Cs_2CO_3 , KOAc	none	100	98 (93)
2	I	Cs_2CO_3 , KOAc	PCy_3	100	99
3	I	Cs_2CO_3 , KOAc	pipecolinic acid	100	51
4	Br	K_2CO_3 , KOAc	none	130	87 (>99)
5	Br	K_2CO_3 , KOAc	PCy_3	130	57
6	Br	K_2CO_3 , KOAc	phen	130	68
7	Br	Cs_2CO_3 , KOAc	bathophen	130	30
8	Br	Cs_2CO_3 , KOAc	bipyridine	130	55

^a Reactions were run on a 0.25 mmol scale in 1 mL of solvent for 24 h. ^b A total of 2 equiv of base was used in each case. When two bases were used together, 1 equiv of each was used. ^c Ligand was added in 8 mol%. ^d Corrected GC yields vs internal standard (dodecane), isolated yields in parenthesis.

2.3.2. Dual Base System

Another distinction of the optimized conditions from the previous methodology devised for the C-H activation of benzoic acids was the requirement of two bases. The initial base screens done with the aryl iodide system showed that the yield plateaued around 50% when any singular base was used (Table 2.2 entries 5-8), and that cesium and potassium bases appeared to be the most beneficial in early screenings. This led us to consider using one equivalent of each of two

different bases in combination (for the total two equivalents of base we had seen to be helpful) may boost reactivity. Indeed, using a combination of bases (Cs_2CO_3 and KOAc in the case of iodides, and K_2CO_3 and KOAc in the case of bromides) appeared to give the best results (Table 2.2, entries 1-4 and 9-12). This could be due to the necessity of OAc to aid in the C-H activation step (previously suggested in Miura's studies), but no conclusive evidence to support or exclude this hypothesis was found.

Table 2.2 Optimization of Base System for Aryl Iodides and Aryl Bromides

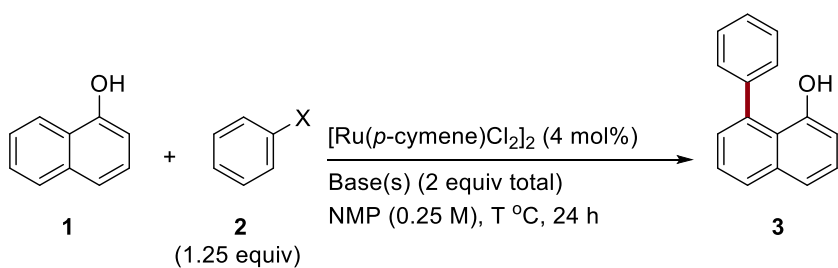
Reaction scheme: 1-naphthol (1) + aryl halide (2) $\xrightarrow[\text{NMP (0.25 M), T } ^\circ\text{C, 24 h}]{[\text{Ru}(p\text{-cymene})\text{Cl}_2]_2 \text{ (4 mol\%)}; \text{Base(s) (2 equiv total)}]$ 1-phenyl-1-naphthol (3)

entry ^a	X	base(s) ^b	T (°C)	yield ^c (%)
1	I	Cs ₂ CO ₃ , KOAc	100	98 (93)
2	I	K ₂ CO ₃ , KOAc	100	91
3	I	K ₂ CO ₃ , CsOAc	100	76
4	I	Cs ₂ CO ₃ , CsOAc	100	90
5	I	Cs ₂ CO ₃	100	51
6	I	K ₂ CO ₃	100	48
7	I	CsOAc	100	28
8	I	KOAc	100	35
9	Br	Cs ₂ CO ₃ , KOAc	130	32
10	Br	K ₂ CO ₃ , KOAc	130	84 (>99)
11	Br	K ₂ CO ₃ , CsOAc	130	46
12	Br	Cs ₂ CO ₃ , CsOAc	130	38
13	Br	Cs ₂ CO ₃	130	48
14	Br	K ₂ CO ₃	130	71
15	Br	CsOAc	130	6
16	Br	KOAc	130	12

^a Reactions were run on a 0.25 mmol scale in 1 mL of solvent for 24 h. ^b A total of 2 equiv of base was used in each case. When two bases were used together, 1 equiv of each was used. ^c Corrected GC yields vs internal standard (dodecane), isolated yields in parenthesis.

In order to attempt to determine the role of the KOAc, which was required for both optimized conditions, we screened various loadings of this base, utilizing the other base to make up for the additional amount required to have two total equivalents of base present (Table 2.3). While screening with one equivalent (standard reaction conditions) of the KOAc and one equivalent of the complimentary base under each set of reaction conditions as well as having only 5 mol% KOAc present with the rest of the total two equivalents of base made from the complimentary base, we found only a slight decrease in yield (roughly 10% in both cases). Though this did not help to determine if KOAc was acting as some sort of ligand under the reaction conditions, it allowed us to make a choice moving forward as to how much of this base we wanted to use. Given that the complimentary base in both sets of conditions was more expensive, we decided for ease of measuring and price point to continue with our bases in a 1:1 ratio in both cases.

Table 2.3 Investigation of KOAc Loading Required

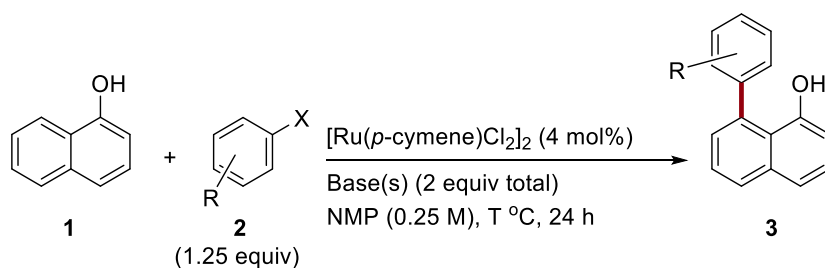


entry ^a	X	base(s) ^b	T (°C)	yield ^c (%)
1	I	CS ₂ CO ₃ , KOAc	100	98
2	I	CS ₂ CO ₃ , KOAc (5 mol%)	100	85
3	Br	K ₂ CO ₃ , KOAc	130	84
4	Br	K ₂ CO ₃ , KOAc (5 mol%)	130	71

^a Reactions were run on a 0.25 mmol scale in 1 mL of solvent for 24 h. ^b A total of 2 equiv of base was used in each case. Unless noted, 1 equiv of each was used. ^c Corrected GC yields vs internal standard (dodecane), isolated yields in parenthesis.

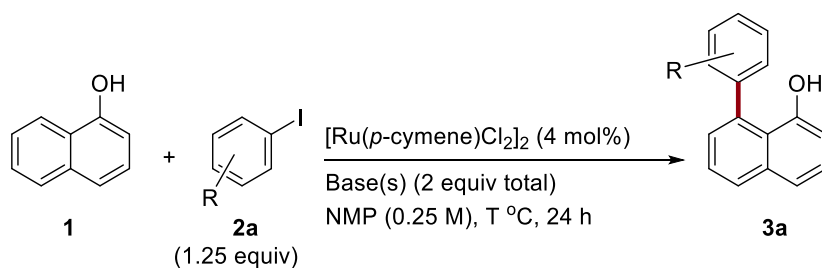
2.3.3. Final Optimized Conditions

The optimal conditions (Table 2.4, entries 1, 10, and 12) do not require an ancillary ligand, but, similar to what Miura reported with palladium catalysis, both a carbonate and acetate base are essential.^{7,2} Aryl bromides and iodides are both coupled under essentially the same conditions, but at lower temperature with cesium carbonate, activated aryl iodides can be coupled while aryl bromides provide low yields (entries 1, 6, 7, and 12). In cases with challenging aryl iodides, the higher-temperature conditions worked best, and these conditions appear to be the most general (Table 2.5). Even though unactivated aryl bromides could be coupled, chlorobenzene could not be coupled (Table 2.4, entry 13).

Table 2.4 Optimized Conditions for the Arylation of 1-Naphthol

entry ^a	X	base(s) ^b	T (°C)	yield ^c (%)
1	I	Cs_2CO_3 , KOAc	100	98 (93)
2	I	KOAc	100	45
3	I	Cs_2CO_3	100	50
4	I ^d	Cs_2CO_3 , KOAc	100	96
5	I ^e	Cs_2CO_3 , KOAc	100	0
6	Br	Cs_2CO_3 , KOAc	100	35
7	Br	K_2CO_3 , KOAc	130	72 (>99)
8	Br	KOAc	130	12
9	Br	K_2CO_3	130	71
10	Br ^d	K_2CO_3 , KOAc	130	75
11	Br ^e	K_2CO_3 , KOAc	130	0
12	I	K_2CO_3 , KOAc	130	96
13	Cl	K_2CO_3 , KOAc	130	6

^a Reactions were run on a 0.25 mmol scale in 1 mL of solvent for 24 h. ^b A total of 2 equiv of base was used in each case. When two bases were used together, 1 equiv of each was used. ^c GC yield vs internal standard (dodecane), isolated yields in parenthesis. ^d 1.5 equiv of aryl halide used. ^e Ruthenium catalyst omitted.

Table 2.5 Aryl Iodides Under Conditions A Versus B

entry ^a	2	base(s) ^b	T (°C)	yield ^c (%)
1	Iodobenzene	Cs ₂ CO ₃ , KOAc	100	91
2	Iodobenzene	K ₂ CO ₃ , KOAc	130	97
3	Iodothiophene	Cs ₂ CO ₃ , KOAc	100	72
4	Iodothiophene	K ₂ CO ₃ , KOAc	130	83

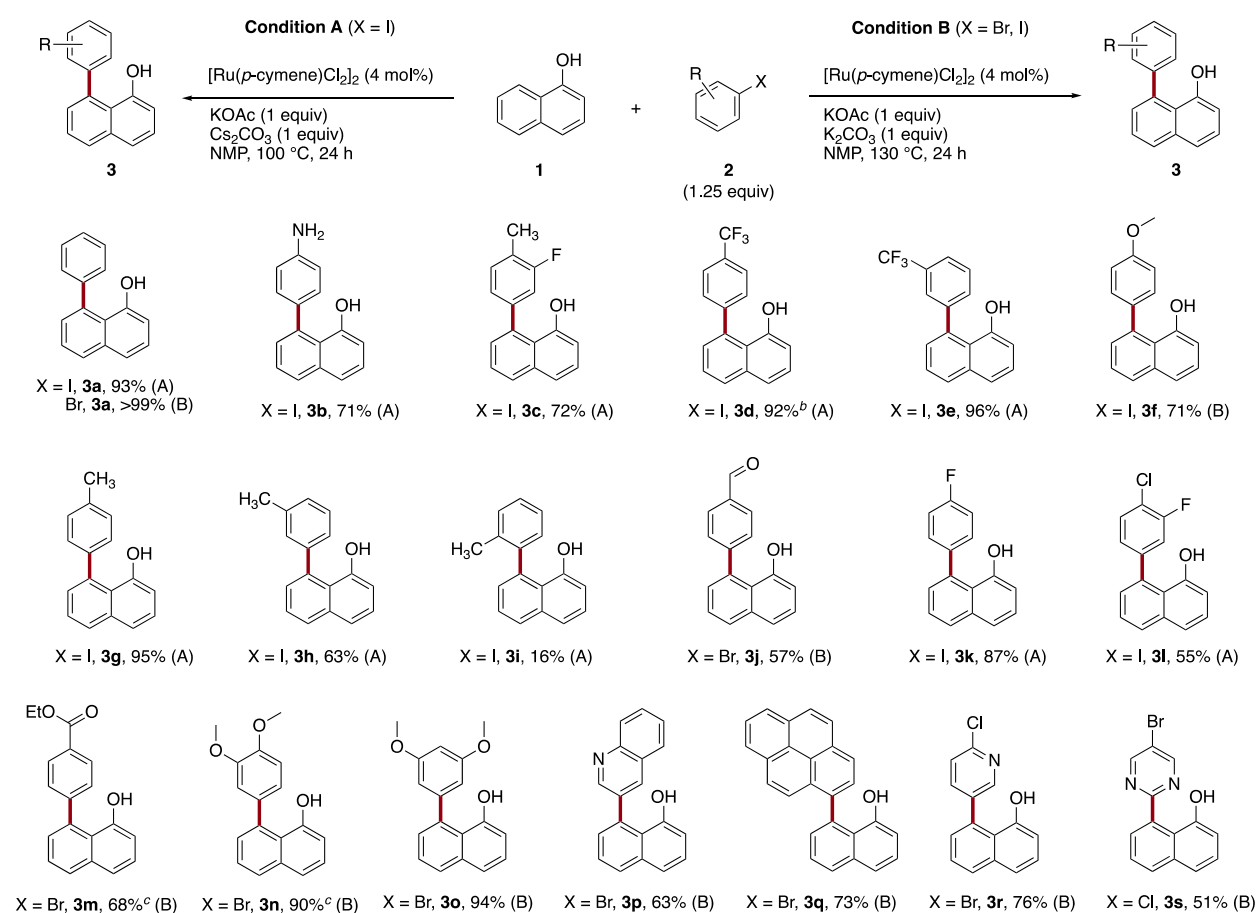
^a Reactions were run on a 0.25 mmol scale in 1 mL of solvent for 24 h. ^b A total of 2 equiv of base was used in each case. When two bases were used together, 1 equiv of each was used. ^c Corrected GC yields vs internal standard (dodecane), isolated yields in parenthesis.

2.3.4. Evaluation of Substrate Scope

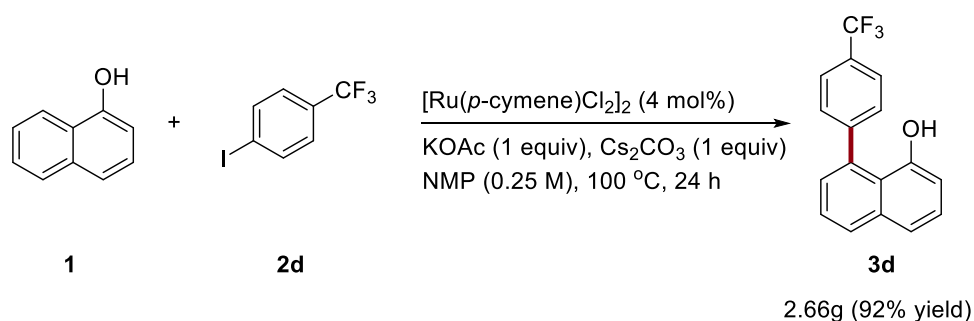
Application of these conditions to a variety of aryl halides is demonstrated in Scheme 2.3. Both electron-rich and electron-poor aryl iodides and bromides can be coupled in useful yields, but for electron-rich aryl iodides the higher temperature conditions were found to be optimal. Important improvements over previously reported methods are tolerance for reactive functional groups: an unprotected aniline (**3b**), an ester (**3m**), and an aldehyde (**3j**); and the ability to couple heteroaryl halides (**3p**, **3r**, **3s**). Substitution at the *ortho*-position of the aryl halide generally resulted in diminished yields (compare **3g** to **3i**), but bromopyrene was coupled in 73% yield (**3q**). In addition, dihalide substrates were also tolerated, with the more reactive carbon-halide bond

being selectively arylated (3l, 3r, 3s), although selectivity was not always perfect, resulting in diminished yields (3s). While chlorobenzene had been unsuccessful (Table 2.4, entry 13), 2-chloropyrimidine was reactive (3s). This selectivity allows for the use of different halides as orthogonal functional group handles for further chemical elaboration. Finally, the reaction could be scaled to 10 mmol scale without difficulty using standard Schlenk techniques (Figure 2.4, 2.66 g of product).

Figure 2.3 Intermolecular C–H Arylation of 1-Naphthol with (Hetero)aromatic Halides^a



^a Reactions were run on a 0.5 mmol scale in 2 mL of solvent for 24 h. ^b Reaction was run on a 10.0 mmol scale using standard Schlenk line techniques on the benchtop. ^c Product was inseparable from a small amount (<8%) of naphthol impurity. The yield has been adjusted based upon NMR.

Figure 2.4 Large Scale Arylation of 1-Naphthol

2.4. Conclusion

While 8-aryl-1-naphthols are promising dye molecules and useful intermediates in the synthesis of polycyclic aromatic hydrocarbons, they can be difficult to access. A new, ruthenium-catalyzed method for peri C-H arylation of 1-naphthol with a variety of aryl and heteroaryl halides (iodides, bromides) is reported that overcomes the limitations of previous palladium-catalyzed approaches. Yields for the 20 examples range from 16-99%, with an average of 71%, and the reaction tolerates a variety of functional groups: pyridine, pyrimidine, primary aniline, aldehyde, and ester.

This new approach to peri-substituted naphthols expands the pool of 8-arylated naphthol derivatives that can be accessed in a single step to include nitrogen-substitution, a common component in some of the most promising dyes.¹⁸ This result mirrors our findings for the arylation of benzoic acids,²⁴⁻²⁷ demonstrating again how ruthenium C-H arylation is a useful complement to palladium catalyzed methods.^{6,10,17}

2.5. Experimental

2.5.1. Materials

Dry NMP (1-Methyl-2-pyrrolidinone, anhydrous, 99.5%) was purchased and used without purification.

2.5.2. General Methods

^1H nuclear magnetic resonance (NMR) spectroscopy chemical shifts are reported in ppm and referenced to TMS (tetramethylsilane) in CDCl_3 ($\delta = 0$ ppm) or the residual solvent peak for CDCl_3 ($\delta = 7.26$ ppm). For ^{13}C NMR and ^{19}F NMR chemical shifts, the residual solvent peak (CDCl_3 , $\delta = 77.00$ ppm) and TMS ($\delta = 0$ ppm) were used as references. Chemical shifts are reported in parts per million (ppm), multiplicities are indicated by s (singlet), d (doublet), t (triplet), q (quartet), m (multiplet) and br (broad). Coupling constants (J) are reported in Hertz.

GC analyses were performed on an Agilent 7890A GC equipped with dual DB-5 columns ($20\text{ m} \times 180\text{ }\mu\text{m} \times 0.18\text{ }\mu\text{m}$), dual FID detectors, and hydrogen as the carrier gas. A sample volume of $1\text{ }\mu\text{L}$ was injected at a temperature of $300\text{ }^\circ\text{C}$ and a 100:1 split ratio. The initial inlet pressure was 20.3 psi but varied as the column flow was held constant at $1.8\text{ mL}/\text{min}$ for the duration of the run. The initial oven temperature of $50\text{ }^\circ\text{C}$ was held for 0.46 min followed by a temperature ramp of $65\text{ }^\circ\text{C}/\text{min}$ up to $300\text{ }^\circ\text{C}$. The temperature was held at $300\text{ }^\circ\text{C}$ for 3 min. The total run time was ~ 7.3 min and the FID temperature was $325\text{ }^\circ\text{C}$.

Chromatography was performed on silica gel (EMD, silica gel 60, particle size 0.040-0.063 mm) using standard flash techniques or on 40 g HP Silica column (catalog 69-2203-347) using a Teledyne Isco Rf- 200 (detection at 210 nm and 340 nm). Products were visualized by UV-vis.

GCMS was done with a Shimadzu GCMS-2010S. For non-volatile compounds, high resolution mass spectra (HRMS) mass spectrometry data was collected on a Thermo Q Exactive™ Plus (ESI-Q-IT-MS) (thermofisher.com) via flow injection with electrospray ionization. An ASAP-MS™ source (ionSence, Saugus, MA) on the Thermo Q Exactive™ Plus was used to obtain HRMS for volatile compounds analyzed by GCMS. This HRMS data was acquired by the chemistry mass spectrometry facility at the University of Wisconsin- Madison.

2.5.3. General Reaction Procedures

2.5.3.1. General Procedure for the Arylation of 1-Naphthol and Aryl Iodides

(Condition A)

Glovebox procedure: On the bench, an oven-dried 1-dram vial fitted with a Teflon-coated stir-bar was charged with [Ru(*p*-cymene)Cl₂]₂ (12.3 mg, 0.02 mmol, 4 mol%), 1-naphthol (72.1 mg, 0.50 mmol, 1.0 equiv), and potassium acetate (49.1 mg, 0.50 mmol, 1.0 equiv). The vial was moved into a nitrogen filled glove box and Cs₂CO₃ (162.9 mg, 0.50 mmol, 1.0 equiv), dodecane (as an internal standard, 10.0 μL), aryl iodide (0.625 mmol, 1.25 equiv), and NMP (2.00 mL) were sequentially added. The vial was capped with a screw cap fitted with a PTFE-faced silicone septum, removed from the glove box, and heated in a reaction block set to 100 °C on the benchtop with stirring at 1250 rpm until the reaction was judged complete (<5% 1-naphthol or aryl iodide remaining) by GC analysis, typically 24 h.

Benchtop procedure: An oven-dried 100 mL Schlenk flask containing a PTFE-coated stir-bar was charged with $[\text{Ru}(p\text{-cymene})\text{Cl}_2]_2$ (0.24 g, 0.4 mmol, 4 mol %), 1-naphthol (1.44 g, 10.0 mmol, 1.0 equiv), potassium acetate (0.98 g, 10.0 mmol, 1.0 equiv), and Cs_2CO_3 (3.26 g, 10.0 mmol, 1.0 equiv). 50 mL of anhydrous NMP was then added to the flask, which was subsequently attached to a nitrogen manifold. The headspace was purged with N_2 (through the stopcock with venting through a needle in the septum). After 10 min, the vent needle was removed from the septum and 4-iodobenzotrifluoride (1.47 mL, 12.5 mmol, 1.25 equiv) was added via syringe. The flow of N_2 into the vessel was turned off and the sealed (septum) reaction vessel was stirred (1250 rpm) in a 100 °C oil bath for 24 h.

2.5.3.2. General Procedure for the Arylation of 1-Naphthol and Aryl Bromides (Condition B)

Glovebox procedure: As for condition A, except that K_2CO_3 (69.1 mg, 0.50 mmol, 1.0 equiv) and aryl bromide (0.625 mmol, 1.25 equiv), and NMP (2.00 mL) were used in place of Cs_2CO_3 and aryl iodide. The reaction was stirred at 130 °C instead of 100 °C.

2.5.3.3. Isolation and purification

Upon reaction completion, the reaction mixture was diluted with dichloromethane (50 mL). The mixture was poured into a separatory funnel and the organic layer was washed with 1 M LiBr (aq) (50 mL), 1 M HCl (aq) (50 mL), and saturated NaCl (aq) (50 mL). The combined aqueous layers were then extracted with dichloromethane (3×30 mL). The combined organic layers were dried over MgSO_4 , filtered, and the filtrate was concentrated under reduced pressure. The resulting residue was purified by column chromatography on silica gel to afford the pure product.

2.5.4. Product Characterization

8-Phenylnaphthalen-1-ol (3a)²⁰ Condition A from iodobenzene (127.5 mg, 69.7 μ L): 93% yield (102.4 mg). Yellow oil. Condition B from bromobenzene (98.1 mg, 66.6 μ L): >99% yield (110.1 mg). Yellow oil. ¹H NMR (400 MHz, CDCl₃) δ 7.87 (dd, J = 8.3, 1.3 Hz, 1H), 7.52 (m, 6H), 7.43 (dt, J = 17.2, 7.6 Hz, 2H), 7.21 (dd, J = 7.1, 1.3 Hz, 1H), 6.91 (dd, J = 7.6, 1.3 Hz, 1H), 5.40 (s, 1H). ¹³C{¹H} NMR (126 MHz, CDCl₃) δ 153.0, 141.4, 136.2, 135.7, 129.5, 129.0, 128.7, 128.6, 128.5, 126.9, 124.8, 121.3, 121.0, 111.8. HRMS (ESI) *m/z* calculated for C₁₆H₁₁O [M-H]⁻ 219.0815, found 219.0814. Our characterization data are consistent with those previously reported.

8-(4-Aminophenyl)naphthalen-1-ol (3b) Condition A from 4-iodoaniline (136.9 mg): 71% yield (83.5 mg). Brick red oil. ¹H NMR (500 MHz, CDCl₃) δ 7.81 (dd, J = 8.3, 1.2 Hz, 1H), 7.47 (dd, J = 8.2, 1.2 Hz, 1H), 7.39 (dt, J = 15.3, 7.5 Hz, 2H), 7.32–7.27 (m, 2H), 7.17 (dd, J = 7.0, 1.3 Hz, 1H), 6.90 (dd, J = 7.5, 1.2 Hz, 1H), 6.83–6.77 (m, 2H), 5.93 (s, 1H), 3.87 (s, 2H). ¹³C{¹H} NMR (126 MHz, CDCl₃) δ 153.4, 146.9, 136.3, 135.7, 130.6, 130.3, 128.7, 128.3, 126.8, 124.9, 121.6, 120.7, 115.2, 111.4. HRMS (ESI) *m/z* calculated for C₁₆H₁₂NO [M-H]⁻ 234.0924, found 234.0923.

8-(3-Fluoro-4-Methylphenyl)naphthalen-1-ol (3c) Condition A from 2-fluoro-4-iodotoluene (147.5 mg): 72% yield (90.8 mg). Amber oil. ¹H NMR (500 MHz, CDCl₃) δ 7.86 (dd, J = 8.2, 1.3 Hz, 1H), 7.51 (dd, J = 8.2, 1.2 Hz, 1H), 7.47–7.38 (m, 2H), 7.33 (t, J = 7.8 Hz, 1H), 7.21–7.18 (m, 2H), 7.18–7.17 (m, 1H), 6.93 (dd, J = 7.6, 1.3 Hz, 1H), 5.41 (s, 1H), 2.38 (d, J = 2.0 Hz, 3H). ¹³C{¹H} NMR (126 MHz, CDCl₃) δ 161.0 (d, J = 248.2 Hz), 152.8, 140.7 (d, J = 7.5 Hz),

135.6, 134.9 (d, $J = 1.8$ Hz), 131.9 (d, $J = 5.7$ Hz), 128.9, 128.5, 126.9, 125.4 (d, $J = 17.2$ Hz), 124.8, 124.8, 121.2, 121.1, 116.3 (d, $J = 22.4$ Hz), 111.9, 14.4 (d, $J = 3.4$ Hz). $^{19}\text{F}\{^1\text{H}\}$ NMR (377 MHz, CDCl_3) δ 9.42. HRMS (ASAP-MS) m/z calculated for $\text{C}_{17}\text{H}_{12}\text{FO}$ $[\text{M} - \text{H}]^-$ 251.0878, found 251.0878.

8-(4-Trifluoromethylphenyl)naphthalen-1-ol (3d)²⁰ Condition A, benchtop procedure (10.0 mmol scale) from 4-iodobenzotrifluoride (3.4 g, 1.84 mL): 92% yield (2.66 g). Brown solid. Mp. 71.4-74.1 °C (lit.²⁰ 72.8-74.0 °C). ^1H NMR (500 MHz, CDCl_3) δ 7.89 (dd, $J = 8.3, 1.3$ Hz, 1H), 7.74 (d, $J = 8.0$ Hz, 2H), 7.62 (d, $J = 8.0$ Hz, 2H), 7.54 (dd, $J = 8.2, 1.2$ Hz, 1H), 7.48 (d, $J = 7.0$ Hz, 1H), 7.47 (d, $J = 7.0$ Hz, 0H), 7.41 (t, $J = 7.8$ Hz, 1H), 7.21 (dd, $J = 7.0, 1.3$ Hz, 1H), 6.90 (dd, $J = 7.5, 1.2$ Hz, 1H), 5.00 (s, 1H). $^{13}\text{C}\{^1\text{H}\}$ NMR (126 MHz, CDCl_3) δ 152.4, 146.16, 146.15, 135.8, 135.4, 130.5 (q, $J = 32.6$ Hz), 129.8, 129.1, 128.8, 127.4 (q, $J = 274.5$ Hz), 126.9, 125.3 (q, $J = 3.8$ Hz), 125.2, 125.0, 121.5, 121.2, 112.0, 29.7. $^{19}\text{F}\{^1\text{H}\}$ NMR (377 MHz, CDCl_3) δ 62.52. HRMS (ESI) m/z calculated for $\text{C}_{17}\text{H}_{10}\text{F}_3\text{O}$ $[\text{M} - \text{H}]^-$ 287.0689, found 287.0688. Our characterization data are consistent with those previously reported.

8-(3-Trifluoromethylphenyl)naphthalen-1-ol (3e)²⁰ Condition A from 3-iodobenzotrifluoride (170.0 mg, 90.1 μL): 96% yield (136.4 mg). Dark brown oil. ^1H NMR (400 MHz, CDCl_3) δ 7.89 (dd, $J = 8.3, 1.1$ Hz, 1H), 7.77 (dd, $J = 7.3, 1.2$ Hz, 1H), 7.70 (dd, $J = 15.6, 7.7$ Hz, 2H), 7.60 (t, $J = 7.7$ Hz, 1H), 7.54 (d, $J = 8.1$ Hz, 1H), 7.48 (d, $J = 7.1$ Hz, 1H), 7.46 (d, $J = 6.9$ Hz, 1H), 7.40 (t, $J = 7.9$ Hz, 1H), 7.22 (dd, $J = 5.9, 1.2$ Hz, 1H), 6.88 (dd, $J = 7.6, 1.2$ Hz, 1H), 4.92 (s, 1H). $^{13}\text{C}\{^1\text{H}\}$ NMR (126 MHz, CDCl_3) δ 152.5, 143.4, 140.2, 136.0, 135.4, 132.8, 130.8 (q, $J = 32.4$ Hz), 129.2, 129.1, 128.8, 126.9, 126.4 (q, $J = 3.8$ Hz), 125.2, 124.7 (q, $J = 3.8$ Hz), 124.4 (q, $J = 273.9$ Hz),

121.6, 121.4, 112.0. $^{19}\text{F}\{^1\text{H}\}$ NMR (377 MHz, CDCl_3) δ 62.39. HRMS (ESI) m/z calculated for $\text{C}_{17}\text{H}_{10}\text{F}_3\text{O}$ $[\text{M}-\text{H}]^-$ 287.0688, found 287.0689. Our characterization data are consistent with those previously reported.

8-(4-Methoxyphenyl)naphthalen-1-ol (3f)²⁰ Condition B from 4-iodoanisole (146.3 mg): 71% yield (88.9 mg). Brick red solid. Mp. 114.2-116.4 °C (lit.²⁰ 114.1-114.9 °C). ^1H NMR (500 MHz, CDCl_3) δ 7.84 (dd, J = 8.2, 1.4 Hz, 1H), 7.49 (dd, J = 8.1, 1.3 Hz, 1H), 7.46 –7.41 (m, 3H), 7.42 –7.36 (m, 1H), 7.18 (dd, J = 7.0, 1.3 Hz, 1H), 7.07 –7.01 (m, 2H), 6.91 (dd, J = 7.6, 1.2 Hz, 1H), 5.65 (s, 1H), 3.89 (s, 3H). $^{13}\text{C}\{^1\text{H}\}$ NMR (126 MHz, CDCl_3) δ 159.9, 153.2, 135.8, 135.7, 133.0, 130.7, 128.7, 128.5, 126.8, 124.9, 121.5, 120.9, 114.4, 111.6, 55.4. HRMS (ESI) m/z calculated for $\text{C}_{17}\text{H}_{13}\text{O}_2$ $[\text{M}-\text{H}]^-$ 249.0921, found 249.0922. Our characterization data are consistent with those previously reported.

8-(4-Methylphenyl)naphthalen-1-ol (3g)²⁰ Condition A from 4-iodotoluene (136.3 mg): 95% yield (111.3 mg). Brown oil. ^1H NMR (400 MHz, CDCl_3) δ 7.85 (d, J = 8.3 Hz, 1H), 7.49 (d, J = 8.1 Hz, 1H), 7.41 (p, J = 8.5, 7.9 Hz, 4H), 7.33 (d, J = 7.7 Hz, 2H), 7.22 –7.16 (m, 1H), 6.91 (d, J = 7.5 Hz, 1H), 5.55 (s, 1H), 2.46 (s, 3H). $^{13}\text{C}\{^1\text{H}\}$ NMR (126 MHz, CDCl_3) δ 153.4, 138.8, 138.3, 136.3, 135.9, 129.9, 129.5, 128.8, 128.7, 127.0, 125.0, 121.6, 121.1, 111.9, 21.5. HRMS (ESI) m/z calculated for $\text{C}_{17}\text{H}_{13}\text{O}$ $[\text{M}-\text{H}]^-$ 233.0972, found 233.0972. Our characterization data are consistent with those previously reported, excepting morphology (lit.²⁰ reports a yellow solid).

8-(3-Methylphenyl)naphthalen-1-ol (3h)²⁰ Condition A from 3-iodotoluene (136.3 mg, 80.3 μL): 63% yield (73.6 mg). Amber solid. Mp. 81.6-84.0 °C. ^1H NMR (500 MHz, CDCl_3) δ 7.85 (dd, J =

8.2, 1.3 Hz, 1H), 7.51 –7.42 (m, 2H), 7.42 –7.31 (m, 5H), 7.12 (dd, $J = 6.9, 1.3$ Hz, 1H), 6.87 (dd, $J = 7.6, 1.2$ Hz, 1H), 5.54 (s, 1H), 2.08 (s, 3H). $^{13}\text{C}\{^1\text{H}\}$ NMR (126 MHz, CDCl_3) δ 153.4, 140.3, 137.6, 135.6, 135.4, 130.6, 130.0, 129.2, 128.6, 127.6, 126.8, 126.5, 125.1, 121.6, 121.0, 111.4, 20.1. HRMS (ESI) m/z calculated for $\text{C}_{17}\text{H}_{13}\text{O}$ $[\text{M}-\text{H}]^-$ 233.0972, found 233.0971. Our characterization data are consistent with those previously reported, excepting morphology (lit.²⁰ reports a yellow oil).

8-(2-Methylphenyl)naphthalen-1-ol (3i) Condition A from 2-iodotoluene (136.3 mg, 79.5 μL): 59% yield (69.1 mg). Amber oil. ^1H NMR (500 MHz, CDCl_3) δ 7.73 (dd, $J = 8.2, 1.3$ Hz, 1H), 7.37 (dd, $J = 8.2, 1.2$ Hz, 1H), 7.35 –7.30 (m, 1H), 7.30 –7.25 (m, 2H), 7.25 –7.18 (m, 2H), 7.00 (dd, $J = 7.0, 1.3$ Hz, 1H), 6.77 (dd, $J = 7.6, 1.2$ Hz, 1H), 5.45 (s, 1H), 1.96 (s, 3H). $^{13}\text{C}\{^1\text{H}\}$ NMR (126 MHz, CDCl_3) δ 153.4, 140.3, 137.6, 135.7, 135.4, 130.7, 130.0, 129.2, 128.6, 127.3, 126.9, 126.5, 125.2, 121.7, 121.0, 111.4, 20.2. HRMS (ESI) m/z calculated for $\text{C}_{17}\text{H}_{13}\text{O}$ $[\text{M}-\text{H}]^-$ 233.0972, found 233.0972.

4-(8-hydroxynaphthalen-1-yl)benzaldehyde (3j) Condition B from 4-bromobenzaldehyde (115.6 mg): 57% yield (71 mg). Pale yellow oil. ^1H NMR (500 MHz, CDCl_3) δ 8.03 –7.98 (m, 2H), 7.85 (dd, $J = 8.3, 1.2$ Hz, 1H), 7.56 –7.52 (m, 2H), 7.49 (dd, $J = 8.1, 1.1$ Hz, 1H), 7.43 (dd, $J = 8.3, 7.0$ Hz, 1H), 7.37 (t, $J = 7.8$ Hz, 1H), 7.18 (dd, $J = 7.0, 1.3$ Hz, 1H), 6.90 (dd, $J = 7.6, 1.2$ Hz, 1H), 5.75 (s, 1H). $^{13}\text{C}\{^1\text{H}\}$ NMR (126 MHz, CDCl_3) δ 200.4, 162.9, 137.2, 136.3, 130.6, 129.3, 128.1, 127.3, 126.4, 126.3, 124.9, 124.3, 123.5, 116.8, 111.5. HRMS (ASAP-MS) m/z calculated for $\text{C}_{17}\text{H}_{11}\text{O}_2$ $[\text{M}-\text{H}]^-$ 247.0765, found 247.0764.

8-(4-Fluorophenyl)naphthalen-1-ol (3k) Condition A from 4-fluoriodobenzene (138.8 mg, 72.1 μL): 87% yield (103.6 mg). Brown oil. ^1H NMR (500 MHz, CDCl_3) δ 7.74 (dd, $J = 8.3, 1.2$ Hz, 1H), 7.39 (dd, $J = 8.2, 1.2$ Hz, 1H), 7.37–7.31 (m, 3H), 7.29 (t, $J = 7.3$ Hz, 1H), 7.12–7.04 (m, 3H), 6.79 (dd, $J = 7.6, 1.2$ Hz, 1H), 5.21 (s, 1H). $^{13}\text{C}\{^1\text{H}\}$ NMR (101 MHz, CDCl_3) δ 162.8 (d, $J = 248.6$ Hz), 152.9, 137.5 (d, $J = 3.6$ Hz), 135.8, 135.3, 131.3 (d, $J = 8.1$ Hz), 128.9 (d, $J = 1.2$ Hz), 127.0, 125.0, 121.4, 121.2, 115.8 (d, $J = 21.5$ Hz), 111.9. $^{19}\text{F}\{^1\text{H}\}$ NMR (377 MHz, CDCl_3) δ -113.13. HRMS (ESI) m/z calculated for $\text{C}_{16}\text{H}_{10}\text{FO}$ $[\text{M}-\text{H}]^-$ 237.0721, found 237.0722.

8-(2-Fluoro-4-bromophenyl)naphthalen-1-ol (3l) Condition A from 1-chloro-2-fluoro-4-iodobenzene (160.3 mg, 79.8 μL): 55% yield (74.9 mg). Brown oil. ^1H NMR (500 MHz, CDCl_3) δ 7.85 (dd, $J = 8.3, 1.2$ Hz, 1H), 7.50 (d, $J = 8.2$ Hz, 1H), 7.47–7.41 (m, 2H), 7.37 (t, $J = 7.8$ Hz, 1H), 7.25 (dd, $J = 9.5, 2.0$ Hz, 1H), 7.17 (dt, $J = 7.9, 1.8$ Hz, 2H), 6.86 (dd, $J = 7.6, 1.2$ Hz, 1H), 5.18 (s, 1H). $^{13}\text{C}\{^1\text{H}\}$ NMR (126 MHz, CDCl_3) δ 157.5 (d, $J = 250.8$ Hz), 152.3, 135.8, 134.6, 130.3, 129.1, 128.7, 126.8, 125.8 (d, $J = 3.6$ Hz), 125.0, 121.4, 121.2, 117.8 (d, $J = 21.2$ Hz), 111.9. $^{19}\text{F}\{^1\text{H}\}$ NMR (377 MHz, CDCl_3) δ -114.70. HRMS (ESI) m/z calculated for $\text{C}_{16}\text{H}_9\text{ClOF}$ $[\text{M}-\text{H}]^-$ 271.0331, found 271.0331.

8-(4-Ethylbenzoate)naphthalen-1-ol (3m) Condition B from ethyl 4-bromobenzoate (143.2 mg, 102.0 μL): 68% yield (99.4 mg). This compound could not be separated from a small amount of 1-naphthol. The yield reported has been adjusted to account for this impurity based upon ^1H NMR integration. Light brown solid. Mp. 132.4–133.0 $^\circ\text{C}$. ^1H NMR (500 MHz, CDCl_3) δ 8.21–8.13 (m, 2H), 7.88 (dd, $J = 8.2, 1.2$ Hz, 1H), 7.61–7.56 (m, 2H), 7.55–7.51 (m, 1H), 7.46 (dd, $J = 8.3, 7.0$ Hz, 1H), 7.41 (t, $J = 7.9$ Hz, 1H), 7.21 (dd, $J = 7.0, 1.3$ Hz, 1H), 6.91 (dd, $J = 7.5, 1.2$ Hz, 1H),

5.12 (s, 1H), 4.43 (q, $J = 7.1$ Hz, 2H), 1.43 (t, $J = 7.2$ Hz, 3H). $^{13}\text{C}\{^1\text{H}\}$ NMR (126 MHz, CDCl_3) δ 166.2, 152.6, 146.7, 135.7, 135.6, 130.2, 129.8, 129.7, 129.4 (d, $J = 3.5$ Hz), 129.1, 128.5, 126.9, 124.9, 121.3, 121.2, 112.0, 61.2, 14.4. HRMS (ASAP-MS) m/z calculated for $\text{C}_{19}\text{H}_{15}\text{O}_3$ $[\text{M}-\text{H}]^-$ 291.1027, found 291.1026.

8-(3,4-dimethoxyphenyl)naphthalen-1-ol (3n) Condition B from 4-bromoveratrole (135.7 mg, 89.9 μL): 90% yield (126.0 mg). This compound could not be separated from a small amount of 1-naphthol. The yield reported has been adjusted to account for this impurity based upon ^1H NMR integration. Amber oil. ^1H NMR(500 MHz, CDCl_3) δ 7.85 (dd, $J = 8.3, 1.3$ Hz, 1H), 7.49 (dd, $J = 8.2, 1.2$ Hz, 1H), 7.47–7.36 (m, 2H), 7.22 (dd, $J = 6.9, 1.3$ Hz, 1H), 6.93 (dd, $J = 7.6, 1.2$ Hz, 1H), 6.62 (d, $J = 2.3$ Hz, 2H), 6.57 (t, $J = 2.3$ Hz, 1H), 5.84 (s, 1H), 3.82 (s, 6H). $^{13}\text{C}\{^1\text{H}\}$ NMR (126 MHz, CDCl_3) δ 153.2, 149.3, 149.1, 135.8, 135.7, 133.3, 128.64, 128.58, 126.9, 124.8, 121.6, 120.9, 112.6, 111.7, 111.3, 56.02, 55.99. HRMS (ESI) m/z calculated for $\text{C}_{18}\text{H}_{15}\text{O}_3$ $[\text{M}-\text{H}]^-$ 279.1027, found 279.1026.

8-(3,5-dimethoxyphenyl)naphthalen-1-ol (3o) Condition B from 1-bromo-3,5-dimethoxybenzene (135.7 mg): 94% yield (131.7 mg). Brown oil. ^1H NMR (500 MHz, CDCl_3) δ 7.86 (dd, $J = 8.3, 0.9$ Hz, 1H), 7.52–7.47 (m, 1H), 7.46–7.37 (m, 2H), 7.27–7.20 (m, 1H), 6.93 (dd, $J = 7.6, 1.1$ Hz, 1H), 6.63 (d, $J = 2.3$ Hz, 2H), 6.57 (t, $J = 2.3$ Hz, 1H), 5.81 (s, 1H), 3.82 (s, 6H). $^{13}\text{C}\{^1\text{H}\}$ NMR (126 MHz, CDCl_3) δ 161.0, 153.0, 143.3, 136.0, 135.6, 128.8, 127.9, 126.9, 124.8, 121.2, 120.9, 112.0, 107.4, 100.7, 55.5. HRMS (ASAP-MS) m/z calculated for $\text{C}_{18}\text{H}_{15}\text{O}_3$ $[\text{M}-\text{H}]^-$ 279.1027, found 279.1027.

8-(Quinolin-3-yl)naphthalen-1-ol (3p) Condition B from 3-bromoquinoline (130.0 mg, 84.8 μ L): 63% yield (85.5 mg). Amber oil. ^1H NMR (400 MHz, CDCl_3) δ 8.14 (d, $J = 9.0$ Hz, 1H), 8.06 (d, $J = 8.3$ Hz, 1H), 7.91 (d, $J = 8.2$ Hz, 1H), 7.77 (d, $J = 8.3$ Hz, 3H), 7.60 (t, $J = 7.8$ Hz, 1H), 7.52 (t, $J = 8.1$ Hz, 2H), 7.43 (q, $J = 8.0$ Hz, 2H), 7.36 (d, $J = 7.3$ Hz, 1H), 7.12 (d, $J = 8.9$ Hz, 1H). $^{13}\text{C}\{^1\text{H}\}$ NMR (126 MHz, CDCl_3) δ 162.2, 149.9, 146.6, 140.0, 135.0, 129.8, 128.0, 127.9, 127.5, 127.3, 126.4, 126.1, 125.73, 125.70, 125.0, 124.9, 122.1, 117.3, 112.1. HRMS (ASAP-MS) m/z calculated for $\text{C}_{19}\text{H}_{14}\text{NO}$ $[\text{M}+\text{H}]^+$ 272.1070, found 272.1067.

8-(Pyren-2-yl)naphthalen-1-ol (3q) Condition B from 1-bromopyrene (175.7 mg): 73% yield (125.7 mg). Off-white solid. Mp. 90.4-91.6 $^{\circ}\text{C}$. ^1H NMR (500 MHz, benzene- d_6) δ 8.46 (d, $J = 9.2$ Hz, 1H), 7.99 (d, $J = 8.2$ Hz, 1H), 7.92 (d, $J = 7.6$ Hz, 2H), 7.89 –7.78 (m, 6H), 7.78 –7.66 (m, 4H), 7.61 (d, $J = 8.9$ Hz, 1H), 7.49 (d, $J = 8.1$ Hz, 1H). $^{13}\text{C}\{^1\text{H}\}$ NMR (126 MHz, benzene- d_6) δ 131.23, 131.2, 131.0, 130.6, 129.9, 129.8, 129.0, 127.9, 127.74, 127.68, 127.6, 127.5, 126.3, 126.0, 125.9, 125.7, 125.6, 125.5, 124.93, 124.91, 124.2, 119.9. HRMS (ASAP-MS) m/z calculated for $\text{C}_{26}\text{H}_{15}\text{O}$ $[\text{M}-\text{H}]^-$ 343.1128, found 343.1127. The product was not sufficiently soluble in CDCl_3 to obtain a ^{13}C NMR spectrum with sufficient signal to noise.

8-(2-Chloro-pyridin-5-yl)naphthalen-1-ol (3r) Condition B from 5-bromo-2-chloropyridine (120.3 mg): 76% yield (97.2 mg). Amber oil. ^1H NMR (500 MHz, CDCl_3) δ 8.19 (d, $J = 2.5$ Hz, 1H), 7.93 (dd, $J = 8.4, 1.2$ Hz, 1H), 7.88 (dd, $J = 8.1, 1.3$ Hz, 1H), 7.79 –7.70 (m, 2H), 7.55 –7.40 (m, 3H), 7.22 (dd, $J = 7.5, 1.0$ Hz, 1H), 6.86 (d, $J = 8.7$ Hz, 1H, OH, exchangeable in D_2O). $^{13}\text{C}\{^1\text{H}\}$ NMR (126 MHz, CDCl_3) δ 163.1, 149.6, 148.6, 142.0, 135.0, 128.0, 127.3, 126.5,

126.3, 125.7, 125.4, 121.8, 117.2, 113.5, 112.4. HRMS (ESI) m/z calculated for $C_{15}H_9ClNO$ [$M - H$]⁻ 254.0378, found 254.0380.

8-(3-Bromo-pyrimidin-5-yl)naphthalen-1-ol (3s) Condition B from 5-bromo-2-chloropyrimidine (120.9 mg): 51% yield (65.5 mg). Amber oil. ¹H NMR (500 MHz, CDCl₃) δ 8.55 (s, 2H), 7.93 –7.86 (m, 2H), 7.82 –7.77 (m, 1H), 7.51 (ddd, J = 8.5, 7.1, 1.7 Hz, 2H), 7.46 (ddd, J = 8.2, 6.8, 1.3 Hz, 1H), 7.30 (dd, J = 7.5, 1.0 Hz, 1H). ¹³C{¹H} NMR (126 MHz, CDCl₃) δ 164.4, 160.2, 148.7, 134.8, 128.1, 126.9, 126.5, 126.5, 126.1, 125.6, 121.5, 117.7, 113.2. HRMS (ASAP-MS) m/z calculated for $C_{14}H_8BrN_2O$ [$M+H$]⁺ 300.9971, found 300.9977.

References

- (1) Ackermann, L. *Modern Arylation Methods*; Wiley-VCH: Weinheim, 2009; 543 pp.
- (2) Chen, X.; Engle, K. M.; Wang, D. -H.; Yu, J. -Q. Palladium(II)-catalyzed C-H activation/C-C cross-coupling reactions: versatility and practicality. *Angew. Chem. Int. Ed.* 2009, *48*, 5094.
- (3) Kuhl, N.; Hopkinson, M.N.; Wencel-Delord, J.; Glorius, F. Beyond directing groups: transition-metal-catalyzed C-H activation of simple arenes. *Angew. Chem. Int. Ed.* 2012, *51*, 10236.
- (4) Lyons, T. W.; Sanford, M. S. Palladium-Catalyzed Ligand-Directed C-H Functionalization Reactions. *Chem. Rev.* 2010, *110*, 1147.
- (5) Ackermann, L. Carboxylate-Assisted Transition-Metal-Catalyzed C-H Bond Functionalizations: Mechanism and Scope. *Chem. Rev.* 2011, *111*, 1315-1345.
- (6) Arockiam, P. B.; Bruneau, C.; Dixneuf, P. H. Ruthenium(II)-Catalyzed C-H Bond Activation and Functionalization. *Chem. Rev.* 2012, *112*, 5879-5918.
- (7) Rouquet, G.; Chatani, N. Catalytic Functionalization of C(sp²)-H and C(sp³)-H Bonds by Using Bidentate Directing Groups. *Angew. Chem. Int. Ed.* 2013, *52*, 11726.
- (8) Zhao, Q.; Poisson, T.; Pannecoucke, X.; Besset, T. The Transient Directing Group Strategy: A New Trend in Transition-Metal-Catalyzed C-H Bond Functionalization. *Synthesis* 2017, *49*, 4808.
- (9) Font, M.; Quibell, J. M.; Perry, G. J. P.; Larrosa, I. The use of carboxylic acids as traceless directing groups for regioselective C-H bond functionalization. *Chem. Commun.* 2017, *53*, 5584.
- (10) Nareddy, P.; Jordan, F.; Szostak, M. Recent Developments in Ruthenium-Catalyzed C-H Arylation: Array of Mechanistic Manifolds. *ACS Catalysis* 2017, *7*, 5721-5745.
- (11) McMurray, L.; O'Hara, F.; Gaunt, M. Recent developments in natural product synthesis using metal-catalysed C-H bond functionalization. *J. Chem. Soc. Rev.* 2011, *40*, 1885.

- (12) Yamaguchi, J.; Yamaguchi, A. D.; Itami, K. C-H bond functionalization: emerging synthetic tools for natural products and pharmaceuticals. *Angew. Chem. Int. Ed.* 2012, *51*, 8960.
- (13) Chen, D. Y. K.; Youn, S. W. C-H Activation: A Complementary Tool in the Total Synthesis of Complex Natural Products. *Chem. -Eur. J.* 2012, *18*, 9452.
- (14) Wencel-Delord, J.; Glorius, F. C-H bond activation enables the rapid construction and late-stage diversification of functional molecules. *Nat. Chem.* 2013, *5*, 369.
- (15) Segawa, Y.; Maekawa, T.; Itami, K. Synthesis of Extended π -Systems through C-H Activation. *Angew. Chem. Int. Ed.* 2015, *54*, 66.
- (16) Cernak, T.; Dykstra, K.D.; Tyagarajan, S.; Vachal, P.; Krska, S. W. The medicinal chemist's toolbox for late stage functionalization of drug-like molecules. *Chem. Soc. Rev.* 2016, *45*, 546.
- (17) Seki, M. A New Catalytic System for Ru-Catalyzed C-H Arylation Reactions and Its Application in the Practical Syntheses of Pharmaceutical Agents. *Org. Process Res. Dev.* 2016, *20*, 867.
- (18) Mun, S. Y.; Lee, B. S.; Park, J. C.; Ji, H. S.; Lee, S. H.; Kwon, J. T., Compound For Organic Electronic Element, Organic Electronic Element Using The Same, And An Electronic Device Thereof. Korean Patent KR20140170768, Feb 12, 2014. US Patent US 2016/0005981 A1, Jan. 7, 2016.
- (19) Yamaguchi, M.; Higuchi, M.; Tazawa, K.; Manabe, K. Three-Step Synthesis of Fluoranthenes through Pd-Catalyzed Inter- and Intramolecular C-H Arylation. *J. Org. Chem.* 2016, *81*, 3967.
- (20) Cadman, C. J.; Croft, A. K. Anion- π interactions influence pKa values. *Beilstein J. Org. Chem.* 2011, *7*, 320-328.
- (21) Satoh, T.; Kawamura, Y.; Miura, M.; Nomura, M. Palladium-Catalyzed Regioselective Mono- and Diarylation Reactions of 2-Phenylphenols and Naphthols with Aryl Halides. *Angew. Chem. Int. Ed.* 1997, *36*, 1740.
- (22) Satoh, T.; Inoh, J. -I.; Kawamura, Y.; Miura, M.; Nomura, M. Regioselective Arylation Reactions of Biphenyl-2-ols, Naphthols, and Benzylic Compounds with Aryl Halides under Palladium Catalysis. *Bull. Chem. Soc. Jpn.* 1998, *71*, 2239.
- (23) We could find no examples of naphthol arylation with heteroaryl halides under the palladium-catalyzed conditions from reference 21. We tested the conditions from reference 21 for

substrates 2p and 2s. The reaction with 3-bromoquinoline (2p) (for which the corresponding iodide is not commercially available) resulted in no formation of the C-H arylated product. The reaction with 5-bromo-2-chloropyrimidine (2s) gave a 14% yield (NMR yield versus ferrocene as an internal standard).

- (24) Huang, L.; Weix, D. J. Ruthenium-Catalyzed C–H Arylation of Diverse Aryl Carboxylic Acids with Aryl and Heteroaryl Halides. *Org. Lett.* 2016, *18*, 5432-5435.
- (25) Biafora, A.; Krause, T.; Hackenberger, D.; Belitz, F.; Gooßen, L. J. Ortho-C–H Arylation of Benzoic Acids with Aryl Bromides and Chlorides Catalyzed by Ruthenium. *Angew. Chem., Int. Ed.* 2016, *55*, 14752-14755.
- (26) Mei, R.; Zhu, C.; Ackermann, L. Ruthenium(II)-catalyzed C–H functionalizations on benzoic acids with aryl, alkenyl and alkynyl halides by weak-O-coordination. *Chem. Commun.* 2016, *52*, 13171-13174.
- (27) Simonetti, M.; Cannas, D. M.; Panigrahi, A.; Kujawa, S.; Kryjewski, M.; Xie, P.; Larrosa, I. Ruthenium-Catalyzed C–H Arylation of Benzoic Acids and Indole Carboxylic Acids with Aryl Halides. *Chem.–Eur. J.* 2017, *23*, 549-553.
- (28) Lee, D.-H.; Kwon, K.-H.; Yi, C. S. Dehydrative C–H Alkylation and Alkenylation of Phenols with Alcohols: Expedient Synthesis for Substituted Phenols and Benzofurans. *J. Am. Chem. Soc.* 2012, *134*, 7325-7328.
- (29) Lee, H.; Mane, M. V.; Ryu, H.; Sahu, D.; Baik, M.-H.; Yi, C. S. Experimental and Computational Study of the (Z)-Selective Formation of Trisubstituted Olefins and Benzo-Fused Oxacycles from the Ruthenium-Catalyzed Dehydrative C–H Coupling of Phenols with Ketones. *J. Am. Chem. Soc.* 2018, *140*, 10289-10296.
- (30) Ackermann, L.; Diers, E.; Manvar, A. Ruthenium-Catalyzed C–H Bond Arylations of Arenes Bearing Removable Directing Groups via Six-Membered Ruthenacycles. *Org. Lett.* 2012, *14*, 1154-1157.
- (31) Neufeldt, S. R.; Sanford, M. S. Controlling Site Selectivity in Palladium-Catalyzed C–H Bond Functionalization. *Acc. Chem. Res.* 2012, *45*, 936.
- (32) Rousseaux, S.; Gorelsky, S. I.; Chung, B. K. W.; Fagnou, K. Investigation of the Mechanism of C(sp³)–H Bond Cleavage in Pd(0)-Catalyzed Intramolecular Alkane Arylation Adjacent to Amides and Sulfonamides. *J. Am. Chem. Soc.* 2010, *132*, 10692.

- (33) Maleckis, A.; Kampf, J. W.; Sanford, M. S. A Detailed Study of Acetate-Assisted C–H Activation at Palladium(IV) Centers. *J. Am. Chem. Soc.* 2013, *135*, 6618.
- (34) Shan, C.; Zhu, L.; Qu, L.-B.; Bai, R.; Lan, Y. Mechanistic view of Ru-catalyzed C–H bond activation and functionalization: computational advances. *Chem. Soc. Rev.* 2018, *47*, 7552-7576.
- (35) Warratz, S.; Kornhaaß, C.; Cajaraville, A.; Niepötter, B.; Stalke, D.; Ackermann, L. Ruthenium(II)-Catalyzed C–H Activation/Alkyne Annulation by Weak Coordination with O₂ as the Sole Oxidant. *Angew. Chem., Int. Ed.* 2015, *54*, 5513-5517.

Chapter 3: Nickel-Catalyzed Cross Electrophile Coupling of Aryl Halides and Redox Active Esters and Ethers

3.1. Abstract

The synthetic community traditionally relies heavily upon carbon nucleophiles for use in carbon-carbon bond-forming reactions.¹⁻⁹ The methodology developed thus requires the use of an extremely limited substrate pool given this dependence on nucleophilic coupling partners. Over the past few decades, cross-electrophile coupling reactions have begun to be studied extensively for their unique advantages and complimentary reactivity to traditional cross coupling reactions, as electrophiles are over 300 times more available than their nucleophilic counterparts.¹⁰⁻¹³ To bolster this field even further, many groups have turned to non-traditional electrophiles in the form of pseudo-halides as well as radical-generating molecules derived from more abundant starting materials for these transformations. The nickel-catalyzed cross-electrophile coupling reactions of both *N*-hydroxyphthalimides (NHP esters) and *N*-alkoxyphthalimides (NAP ethers) with aryl halides are of particular interest in helping to broaden this methodology. Use of these redox active esters and ethers as alkyl radical precursors allows for wider access to potential coupling partners, as these precursors are readily synthesized from carboxylic acids and alcohols, respectively. The proposed nickel-catalyzed cross-electrophile coupling reactions are poised to aid the synthetic community in the construction of new C(sp²)-C(sp³) bonds.

3.2. Introduction

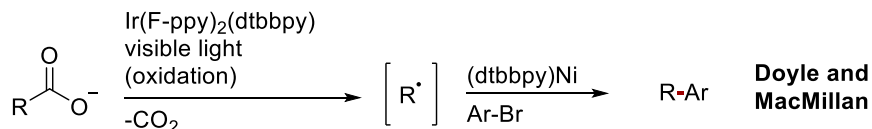
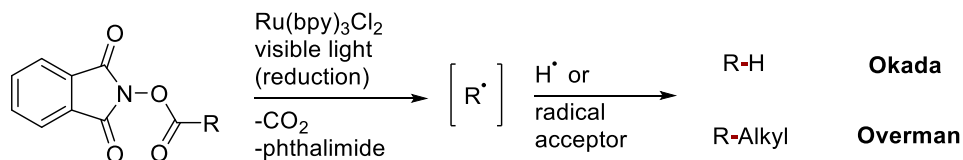
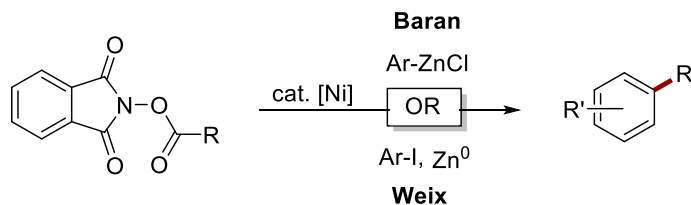
Method development for the formation of C(sp²)-C(sp³) bonds via cross-coupling has advanced rapidly in recent years,¹⁴⁻¹⁷ but continues to remain less advanced than available chemistry for the synthesis of C(sp²)-C(sp²) bonds. One major challenge for these cross-coupling reactions is the lower availability of alkyl coupling reagents compared to aryl coupling reagents.¹⁸ As a potential solution, alkanolic acids and alcohols are much more abundant than alkyl halides, making them attractive coupling partners.¹⁹ While the use of carboxylic acid derivatives as acyl equivalents in cross-coupling has been well-studied,²⁰⁻²¹ few decarboxylative couplings of alkanolic acid derivatives have been reported.²²⁻²³

The emergence and understanding of the radical chemistry required to bolster the development of both C(sp²)-C(sp³) and C(sp²)-C(sp²) bonds has only recently (since around 1970) begun to culminate in methodology development, but was born from robust preliminary discoveries. The discovery of these useful radical processes began with the discovery of the Kolbe electrochemical decarboxylation²⁴, Borodin-Hunsdiecker reaction²⁵⁻²⁶, and the Hofmann-Löffler-Freytag C-H functionalization.²⁷⁻³⁰ These seminal contributions led to the design of alternative radical sources, such as the use of ketyl radicals in the McMurry reaction³¹⁻³² as well as the development of the Kagan reagent.³³⁻³⁵ Following this initial phase of preliminary insight into radical formation, the development of methods that could utilize this new class of synthetic reagents effectively began to thrive. This was due in part to many contributions to the understanding of the mechanistic nuances of radicals in order to allow for rational design of reactions to follow.

First, Gomberg discovered the existence of the trityl radical as a trivalent species³⁶, while Kharasch showed that radicals were capable of accessing anti-Markovnikov selectivity in what would become one of a few early examples of atom-transfer chemistry.³⁷⁻³⁹ Soon after these conclusions had been drawn, Bachmann described what would later be called the persistent radical effect, deducing that coupling between persistent and fleeting radical species should be preferential during a reaction.⁴⁰⁻⁴⁷ This postulation helped lay the foundation for a more informed development of chemical reactions involving the use of radical intermediates.

The field continued to grow through the study of various new radical sources until the late 1960's, when the first of many useful transformations relying on radical species began to be developed. These seminal methods included Mn(III)-mediated oxidative additions to olefins,⁴⁸⁻⁵² radical-cation mediated cycloaddition,⁵³⁻⁵⁴ Minisci heterocycle C-H alkylation⁵⁵⁻⁵⁷ and the beginnings of radical-based cross-coupling chemistry.⁵⁸⁻⁵⁹ The scope of available radical precursors was expanded appreciably again in the late 1980s, with contributions from Hill⁶⁰⁻⁶¹, Zard⁶²⁻⁶⁸, Okada⁶⁹⁻⁷⁰, Nugent and RajanBabu⁷¹⁻⁷³, and Mukaiyama⁷⁴⁻⁷⁵ allowing for the use of more ubiquitous functional groups such as carboxylates, epoxides, and olefins to furnish radicals *in situ*.

Of particular interest to our group, examples of α -heteroatom substituted carboxylates to generate alkyl radical equivalents for use in C(sp²)-C(sp³) bond-forming reactions with aryl halides has been shown recently by the Doyle and MacMillan groups (Figure 3.1a).⁷⁶⁻⁷⁸ However, early examples of the use of activated esters to generate similar radical equivalents have been reported by Okada^{69-70,79-81} and Overman⁸²⁻⁸³, but had not been utilized in metal-catalyzed cross-coupling (Figure 3.1b).

Figure 3.1 Methods for Conversion of Alkanoic Acids to Alkyl Radicals**a) Doyle and MacMillan Visible-Light Carboxylate Chemistry****b) Okada and Overman Visible-Light NHP-Ester Chemistry****c) Weix and Baran Non-photocatalytic Cross-Couplings**

A 2013 study from the Weix group of our alkyl-aryl cross-electrophile coupling (XEC) reaction suggests that an intermediate nickel(II)aryl species can capture alkyl radicals generated from alkyl halides (Figure 3.2).⁸⁴ In 2016, we were able to merge this cross-electrophile coupling with redox active esters in the form of NHP esters, affording cross-coupled products between the alkyl radicals produced and aryl halides.⁸⁵ Upon mechanistic interrogation, it was determined that the radical generation and subsequent bond forming reaction hinged upon the ability of the ligated aryl-Ni complex to facilitate a single electron transfer to the NHP ester, generating an alkyl radical equivalent *in situ*. Given this finding, our group hypothesized redox-active esters (RAEs) such as the NHP ester could generally be used as an alkyl radical precursor under the conditions currently utilized for our XEC reactions involving alkyl halides. This led to the investigation of Barton

esters, as well as Carpino's HOAt and HOBt esters as alkyl halide proxies.⁸⁶⁻⁸⁷ As a result of this postulation, the use of these alkanolic acid derivatives as radical precursors for the formation of C(sp²)-C(sp³) bonds has thrived following initial publications by our group⁸⁵ and the Baran lab (Figure 3.1c).⁸⁸

Given this successful work with NHP esters and other RAEs to deliver alkyl radical equivalents into cross-coupling reactions, we looked to further expand the available substrate pool for XEC reactions by seeking out more sources capable of alkyl radical generation that were complimentary to alkyl halides and the carboxylic acid-derived NHP esters. Within the same timeframe in which our group began to search for new alkyl radical sources compatible with cross-coupling reactions, new methods for the facile generation of alkoxy radicals were being discovered.⁸⁹⁻⁹⁶ Of note, the Chen group reported the first donor-acceptor complex-enabled alkoxy radical generation under mild, metal-free reaction conditions.⁹³ This finding marked the first photocatalyst-free selective C(sp³)-C(sp³) bond cleavage followed by alkylation or allylation. The reaction seemed to be initiated via formation of a donor-acceptor complex between the *N*-alkoxyphthalimide ether and Hantzsch ester *in situ*, leading to a red shift in the overall visible light absorption when compared to the NAP alone.⁹³ This allows for the complex to undergo a visible light-induced electron transfer, forming an *N*-alkoxyphthalimide radical ion, which can eliminate phthalimide and form an alkoxy radical (Figure 3.1b). This alkoxy radical then undergoes β-fragmentation to generate an alkyl radical, which the Chen group subsequently trapped with either allyl or vinyl sulfones to furnish their desired products.

We imagined that the alkyl radical resulting from the Chen work could be harnessed for XEC and posited that the Hantzsch ester would likely not interfere with the generally utilized Ni catalysts or reaction conditions for XEC in our group. Indeed, it seemed reasonable that the

conditions we had established for NHP ester coupling would be tolerant of the added Hantzsch ester and light that might be required to facilitate this transformation. Thus, merging some of the recent conditions under which these NAP ethers could be activated, we looked into the development of conditions for the nickel-catalyzed formation of C(sp²)-C(sp³) bonds via the cross coupling of NAP ethers with aryl halides.

Figure 3.2 Proposed Mechanism for Ni-Catalyzed XEC of Aryl Halides with Alkyl Halides

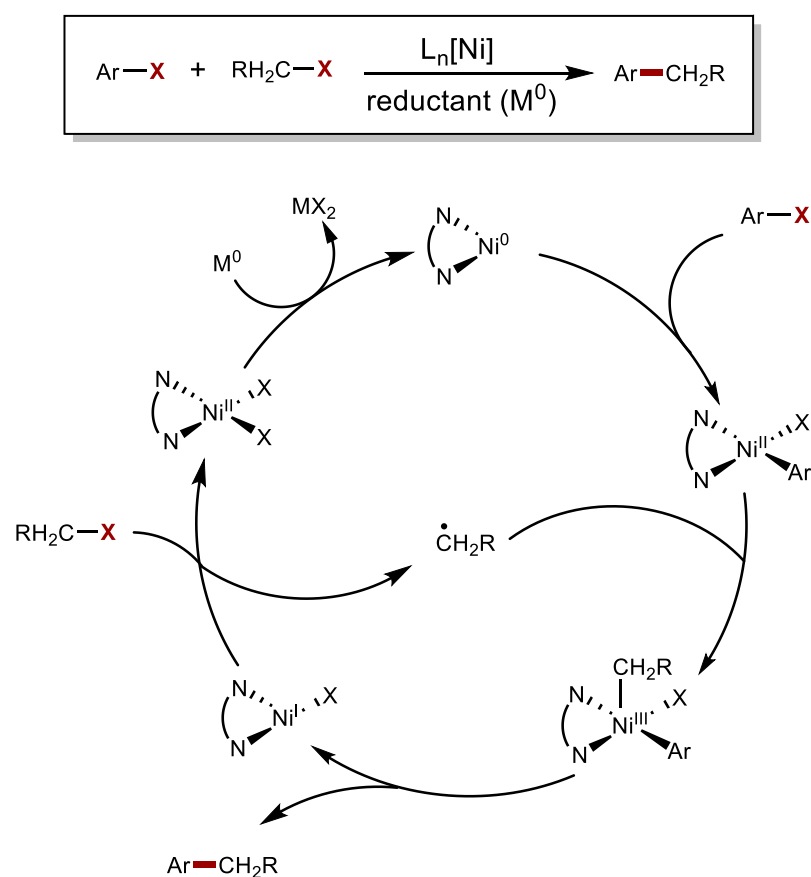
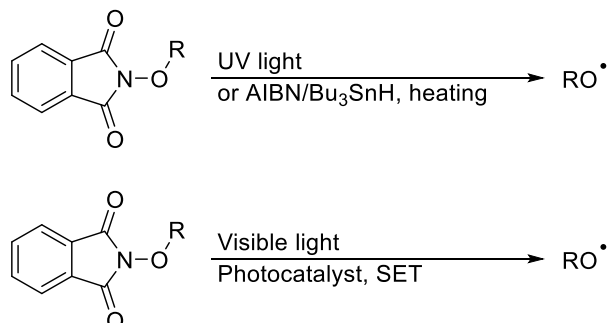
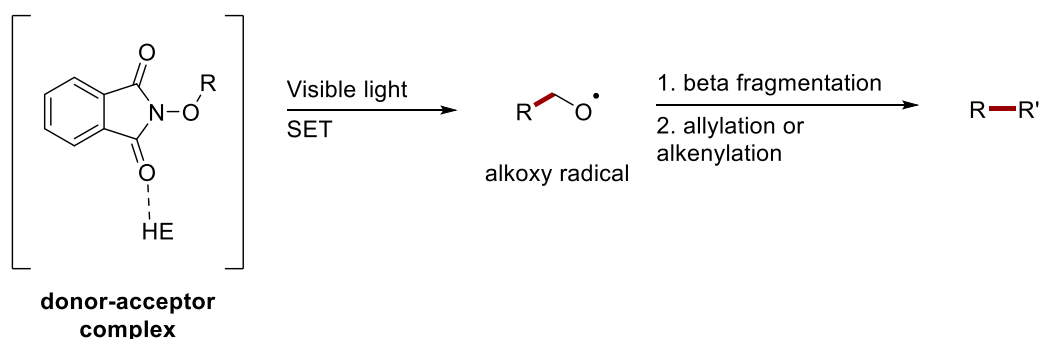


Figure 3.3 Methods for Utilization of *N*-alkoxyphthalimide Ethers in Synthesis**a) Alkoxy radical generation by UV irradiation, heating, or photoredox catalysis****b) Hantzsch ester (HE) enabled alkyl radical generation via donor-acceptor complex**

The generation of oxygen-centered radicals via photo reductive or tin-mediated reductive cleavage of NHP ethers has been known for about two decades (Figure 3.3a).⁸⁹ In recent years, there has been a resurgence of these sorts of reductive radical forming reactions, often in combination with photo redox catalysis.⁹⁰⁻⁹⁵ The alkoxy-radicals generated via these newer methodologies can undergo subsequent β -scission⁹³⁻⁹⁴ to generate carbon-centered alkyl radicals, which have been shown to be viable for capture by standard alkene radical acceptors (Figure 3.3b).

3.3. Results and Discussion

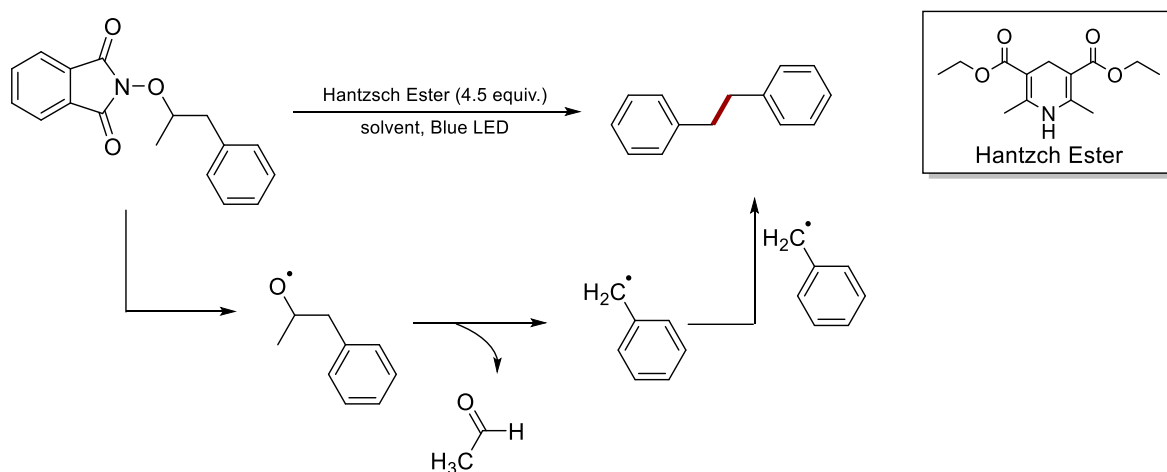
After attempts to find a suitable set of conditions under which the NHP ether chosen could be activated, the model reaction was found to require blue light emitting diodes (LEDs), a nickel catalyst, Hantzsch ester, an amide solvent (*N,N*-dimethylacetamide, DMA), a bidentate amine ligand, and zinc as the terminal reductant. Use of these conditions allowed for a coupling of iodobenzene and a benzylic radical precursor in the form of a NAP ether. Various modifications of this reaction led to a system that allows for the same reaction to proceed in the presence of a nickel catalyst and hemi-labile pyridine-2,6-biscarboximidine (PyBCam) ligand at room temperature with no light or Hantzsch ester required.

3.3.1. Initial Reaction Conditions

To begin an in-depth investigation into conditions that led to the successful coupling of a NAP ether and aryl halide, we hoped to combine conditions from the Chen group⁹³ capable of radical generation with those in our own lab for the subsequent C-C bond formation (Table 3.1).⁸⁵ We first made sure that the NAP ether could be consumed under photochemical conditions in an amide solvent suitable for Weix group XEC, and were pleased to find almost full conversion of the starting material within one hour when the NAP and Hantzsch ester were irradiated via blue LEDs in DMA at room temperature. Interestingly, though some conversion was seen in methanol under photochemical conditions, the starting material seems to be extremely thermally stable, as it showed no decomposition when heated to 100 °C in methanol. With this information in hand, we moved on to see if a Ni(II)Aryl-halide species would be capable of accepting the postulated radical that was being formed in order to generate cross-coupled product. Upon confirmation of

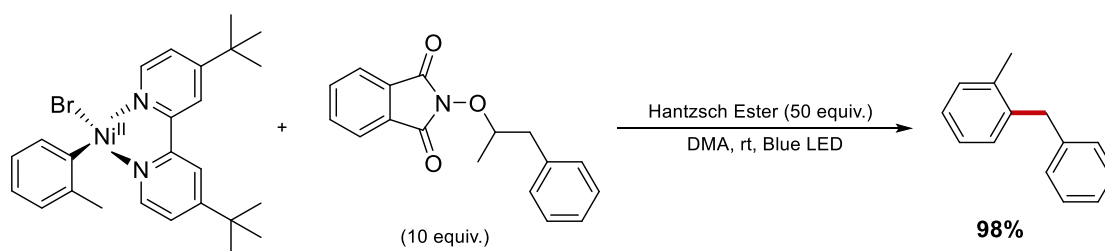
this reactivity (Figure 3.4), we began our optimization by combining the conditions for our previous NHP ester work with those of the Chen group's NAP ether activation (Figure 3.5). This primary reaction yielded the cross-coupled product in 2% and returned all other starting materials after 48 h, but we were hopeful that modifications to the reaction conditions would improve the overall reaction yield.

Table 3.1 Initial Investigation of NAP Ether Activation

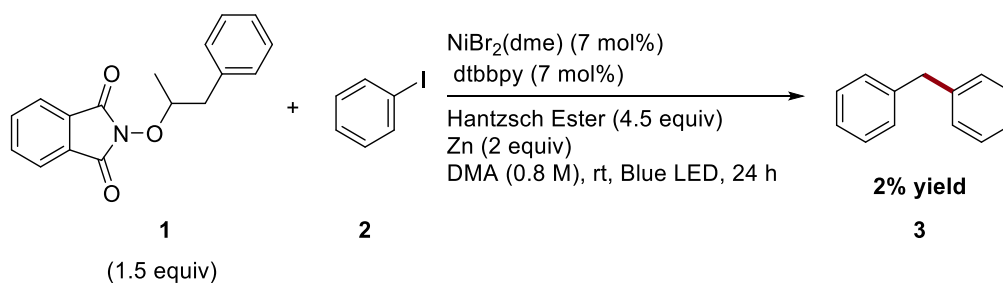


entry ^a	solvent	consumption of NAP ^b (%)
1	methanol	22
2	methanol ^c	nd
3	DMA	98

^aReactions were run on a 0.10 mmol scale in 1 mL of solvent for 1 h. ^bGC consumption vs internal standard (dodecane) based on starting material area. ^cReaction run at 100 °C with omission of Hantzsch ester.

Figure 3.2 Stoichiometric Reaction of Ni(II) Species and NAP Ether

Reaction was run on a 0.40 mmol scale in 0.5 mL of solvent for 24 h. GC yield vs internal standard (dodecane).

Figure 3.3 Initial Catalytic Reaction Conditions

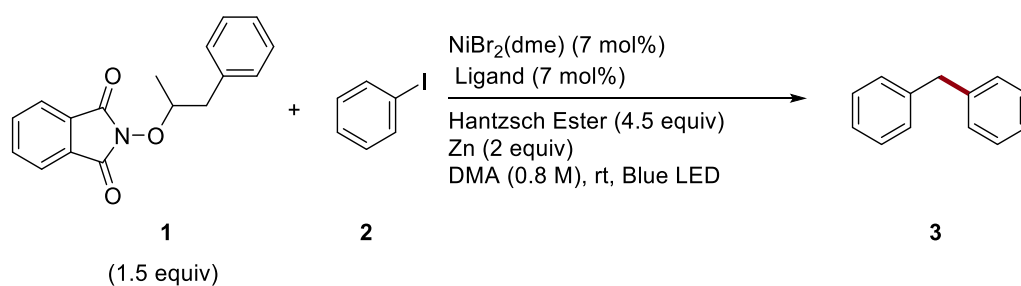
Reaction was run on a 0.40 mmol scale in 0.5 mL of solvent for 24 h. GC yield vs internal standard (dodecane).

3.3.2. Trends with Ligands

Upon looking over the potential reaction conditions available for screening, it was determined that the ligand was likely the best place to start, as our group has found stark changes in both product yield as well as side product distribution when the ligand identity changes in one of our reactions.⁹⁷ With this in mind, a survey of various types and denticities of ligand were interrogated (Table 3.2). Interestingly, the ligand survey showed poor yields and product distributions across the board, with the exception of the newest class of ligand the Weix group has found in collaboration with Pfizer⁹⁸, pyridine-2,6-bis-carboxamidine (PyBCam) (Figure 3.6 and Table 3.2 entry 8). Though all ligands showed full consumption of the NAP ether, which was

reasonable to predict may not be ligand dependent given the prior studies of its decomposition with Hantzsch ester and blue LEDs, significant amounts of bibenzyl (the NAP ether dimer product) and poor consumption of the aryl-iodide seemed to persist in the presence of all ligands investigated.

Table 3.2 Initial Ligand Screen



entry ^a	ligand	yield ^b (%)
1	dtbbpy	2
2	bpy	nd
3	terpy	1
4	phen	nd
5	bathophen	14
6	dppBz	9
7	dppe	6
8	PyBCam	34
9	pyridine	2
10	2-CN-pyridine	nd
11	PPh ₃	3

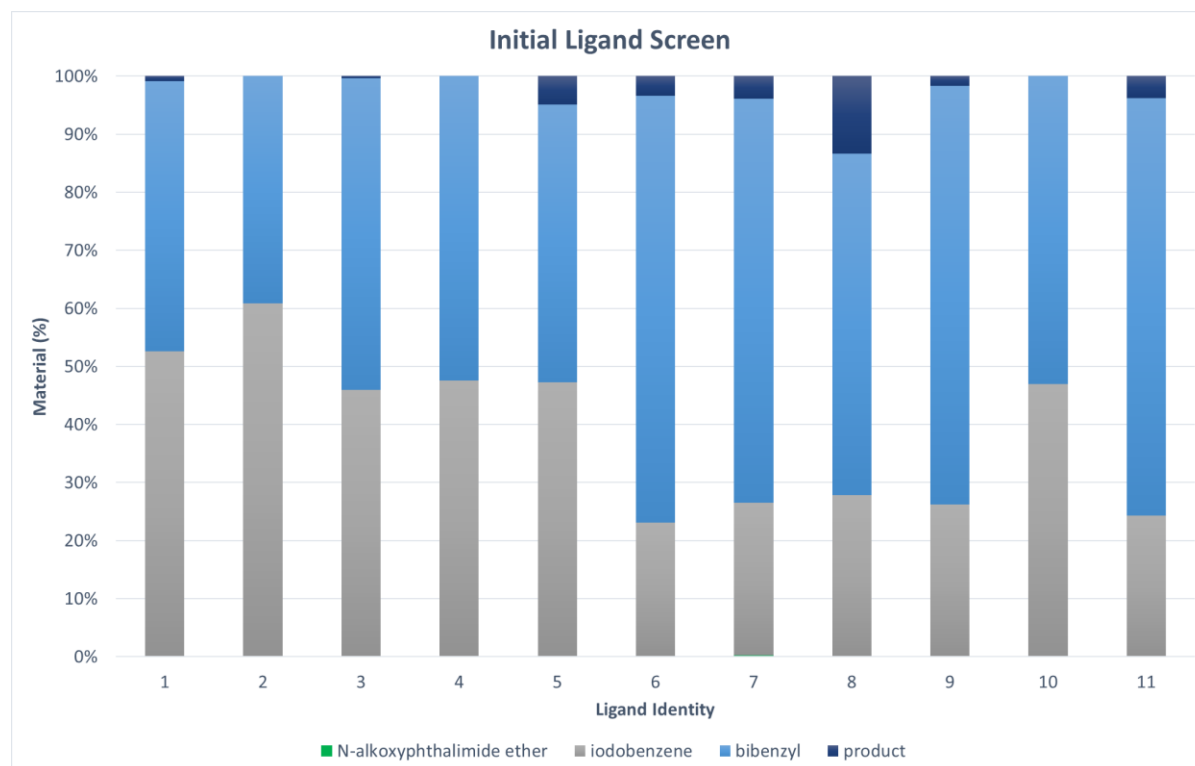
R= H, bipyridine (bpy)
R= t-butyl, dtbbpy

R= H, Phenanthroline (phen)
R= Ph, Bathophenanthroline (Bphen)

dppe

dppBz

^a Reactions were run on a 0.80 mmol scale in 1 mL of solvent for 17 h. ^b GC yield vs internal standard (dodecane).

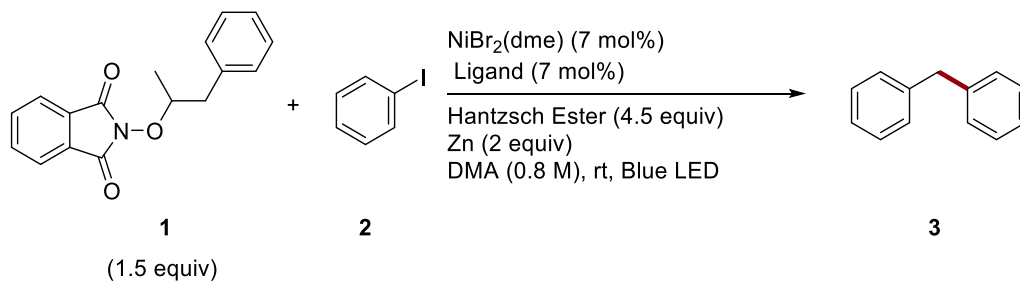
Figure 3.4 Initial Ligand Screen Product Distribution

Reactions were run on a 0.80 mmol scale in 1 mL of solvent for 17 h. GC yield vs internal standard (dodecane).

This increased product yield led us to further investigate this class of pyridine-2,6-biscarboxamidine type ligands (Table 3.3, Figure 3.7). We were pleased to find that all these ligands appeared to outperform our more traditionally useful ligand sets in this chemistry. In all cases, aryl-iodide was completely consumed within 24 h, and the only major biproduct appeared to be that of the NAP ether derived dimer (bibenzyl) for most reactions. A promising result was found in the case of the *para*-methoxy substituted ligand, ^{MeO}PyBCam, as it gave the best overall conversion to product, with the remainder of missing yield being attributed to the dehalogenation of the iodobenzene. It also seemed that the yield of product was linearly related to the relative electronics of the ligands, given that the more electron rich the ligand was, the higher a yield of

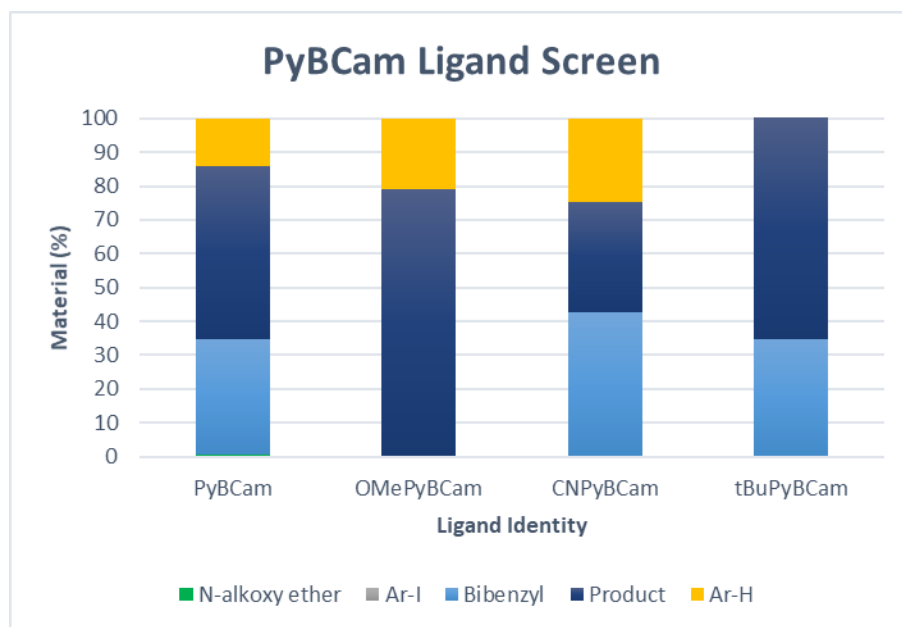
cross-coupled product was formed (entry 1 vs 4 or 4 vs 5). Given the trend, a *para*-dimethylamino analogue of the PyBCam is being synthesized created in hopes to achieve even greater reactivity.⁹⁹

Table 3.3 PyBCam Ligand Family Screen



entry ^a	ligand	σ	yield ^b (%)
1	PyBCam	0.00	51
2	OMePyBCam	-0.27	78
3	CNPyBCam	0.66	33
4	<i>t</i> BuPyBCam	-0.20	66

^a Reactions were run on a 0.80 mmol scale in 1 mL of solvent for 26 h. ^b GC yield vs internal standard (dodecane).

Figure 3.5 PyBCam Ligand Family Product Distribution

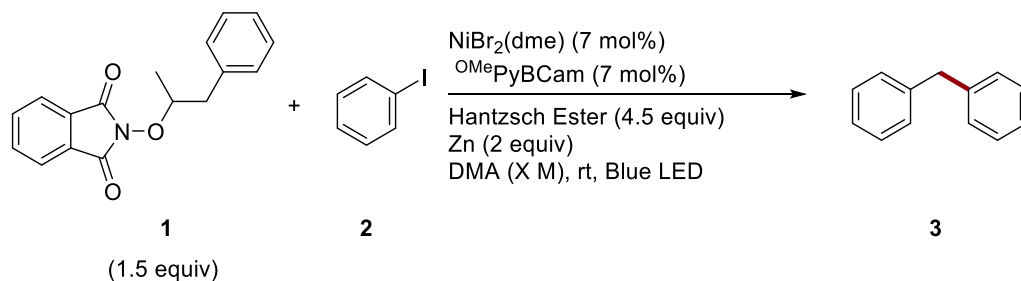
Reactions were run on a 0.80 mmol scale in 1 mL of solvent for 26 h. GC yield vs internal standard (dodecane).

3.3.3. Reaction Concentration Effects

Having chosen the ^{MeO}PyBCam ligand to move forward with, we next looked into the effect of the reaction concentration, positing that it would be fairly important to the overall transformation given that it would affect the overall light penetration through the solution, given that using 4.5 equiv of Hantzsch ester meant that at higher concentrations, not all of it was solubilized towards the beginning of the reaction. Consistent with this hypothesis, it was found that if the reaction were too concentrated, the yield suffered, but anything more dilute than 0.8 M did not seem to make a difference (Table 3.4). While looking into this concentration effect, we also noticed that after 24 h, the reactions seemed complete, giving the 48-hour data shown below that matched the data gathered at 24 h for each of the reactions. It seemed that the reaction was complete at or before 24 h, but given the difference in yield between ligand screens for the

PyBCam ligand (Table 3.3 entry 8 vs Table 3.4 entry 1), it is likely that the reaction takes somewhere between 17 to 24 h to complete.

Table 3.4 Concentration Investigation



entry ^a	reaction concentration	yield ^b (%)
1	1.6 M	43
2	0.8 M	80
3	0.4 M	78

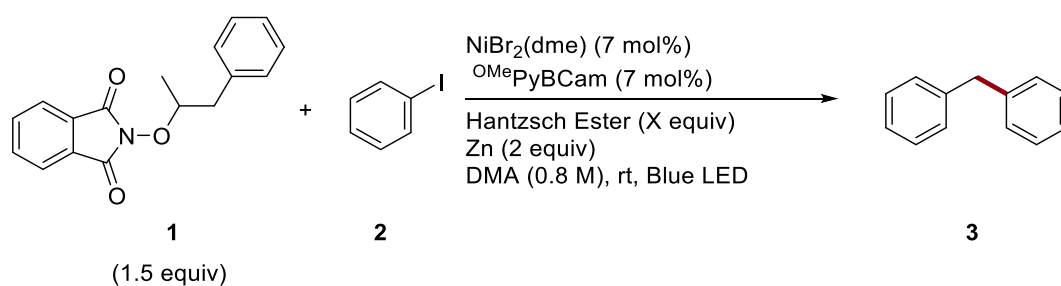
^a Reactions were run on a 0.80 mmol scale in either 0.5, 1, or 2 mL of solvent for 48 h. ^b GC yield vs internal standard (dodecane).

3.3.4. Requirement of Acceptor/Donor Pair

Given the mechanistic hypothesis from the seminal NHP ester work conducted in our group, we had reason to believe that the nickel catalyst might be capable of the single electron transfer (SET) required to activate the NAP ether and subsequently form the alkyl radical. This, coupled with our mechanistic understanding of the overall catalytic cycle for this type of XEC reaction, we further concluded that as long as the catalyst was capable of SET, it would be able to complete the oxidative addition, radical capture, and successive reductive elimination to form the desired product on its own as long as zinc was present as a terminal reductant. Thus, the next

systematic change made to the reaction conditions was to determine if the Hantzsch ester was necessary for this transformation. Gratifyingly, the results were in line with this reasoning, and screening away from the initial 4.5 equiv of Hantzsch ester showed that it was not required in order to facilitate productive chemistry (Table 3.5).

Table 3.5 Determination of the Requirement of Hantzsch Ester



entry ^a	equiv Hantzsch ester	yield ^b (%)
1	none	78
2	0.07	81
3	0.1	83
4	0.5	83
5	1.5	81
6	2.5	83
7	4.5	79

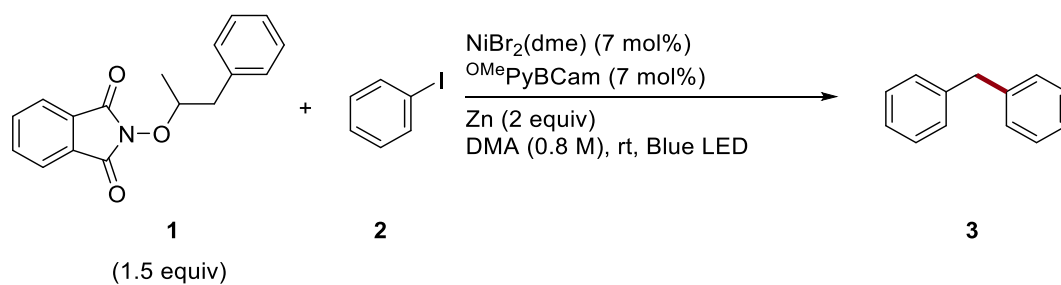
^a Reactions were run on a 0.80 mmol scale in 1 mL of solvent for 24 h. ^b GC yield vs internal standard (dodecane).

3.3.5. Light Requirements

Once it was determined that Hantzsch ester was not required to facilitate the SET to the NAP ether in order to induce β -scission and radical formation, we postulated that the blue LEDs

may not be required for this reaction to proceed either. This conclusion was reached via two pieces of information: 1) the work from the Chen group utilizing Hantzsch ester to form a donor-acceptor pair only required blue LED to excite this pairing, which our conditions no longer had and 2) the work we had previously done utilizing NHP esters involved an insightful stoichiometric reaction between the nickel(II)aryl-halide and the NHP ester that worked in the dark, contrary to previous studies which had also reported the need for light. This meant that our Ni catalyst might be capable of SET to the NAP ether in order to generate the alkyl radical without the need for photochemical conditions, as we had seen with the NHP esters.

Thus, a panel of various amounts of light was investigated, as under the similar conditions for productive Ni-catalyzed NHP ester reactivity, we had already noted that the SET could occur in the absence of light. Here too, we concluded that light was not essential for the reaction to proceed (Table 3.6), as regardless of the light provided to the reaction vessel, the same yield was obtained. We therefore made the decision to run our reactions in ambient light, as it did not require a tailored light set-up to achieve, and there was no reason to use tin foil to omit light altogether.

Table 3.6 Ascertaining the Necessity of Light on Reactivity

entry ^a	deviation	yield ^b (%)
1	none	78
2	ambient light	76
3	dark (foil wrapped)	78

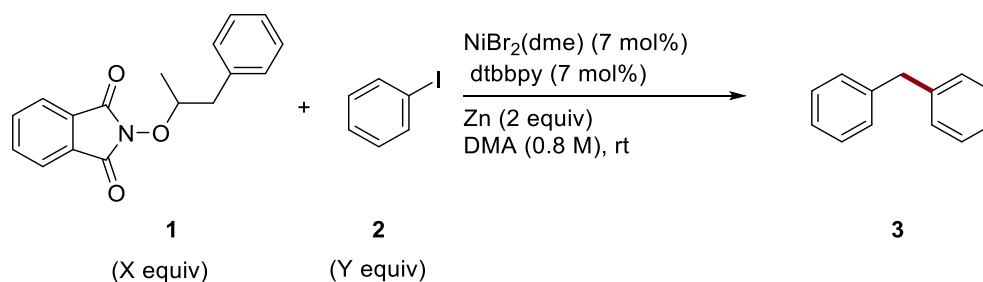
^aReactions were run on a 0.80 mmol scale in 1 mL of solvent for 24 h. ^bGC yield vs internal standard (dodecane).

3.3.6. Optimizing for Ratio of Substrates

The last and most recent set of reaction conditions to be considered was the relative ratio of the two coupling partners. In most reactions, the major side products observed were unreacted aryl halide and biphenyl (the dimer resulting from the aryl halide). After the change to using MeOPyBCam as a ligand, we were no longer observing much bibenzyl formation (the dimer resulting from the NAP ether). It seemed that it may be possible to lower the required amount of NAP ether from 1.5 equiv without disturbing the reaction distribution, which would be advantageous given that this starting material needed to be prepared and was not commercially available. After varying the ratios of the coupling partners however (Table 3.7) we found that the original 1.5:1.0 equiv of NAP ether to aryl iodide was the optimal ratio, giving only a small amount of unreacted starting material and biphenyl after 24 h. In contrast, in all cases where the relative amount of the aryl iodide was increased (Table 3.7, entries 2-5), a drastic increase in unreacted

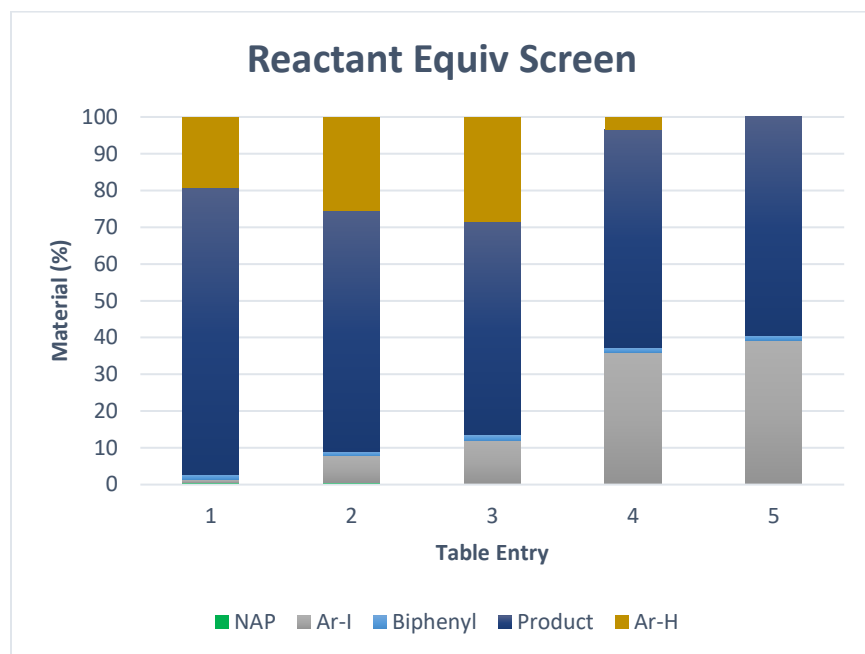
aryl iodide was seen after the NAP ether was fully consumed (Figure 3.8). It would be logical to see if increasing the ratio of NAP ether to aryl iodide from 1.5:1.0 equiv to 1.75:1.0 or 2.0:1.0 equiv would cause consumption of the slight remainder of unreacted aryl iodide seen. However, even in the case that more NAP ether was advantageous, utilizing more than 1.5 equiv of one coupling partner for a slight increase in yield (potentially 4%, as that is on average the amount of returned iodobenzene under the current conditions) might not be the most economic decision.

Table 3.7 Optimization of Substrate Ratio



entry ^a	equiv 1	equiv 2	yield ^b (%)
1	1.5	1.0	78 (78)
2	1.25	1.0	66
3	1.0	1.0	58
4	1.0	1.25	59
5	1.0	1.5	60

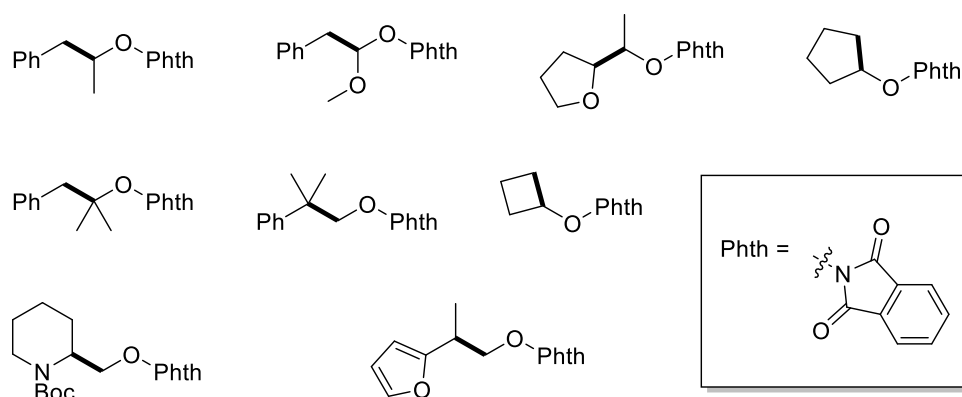
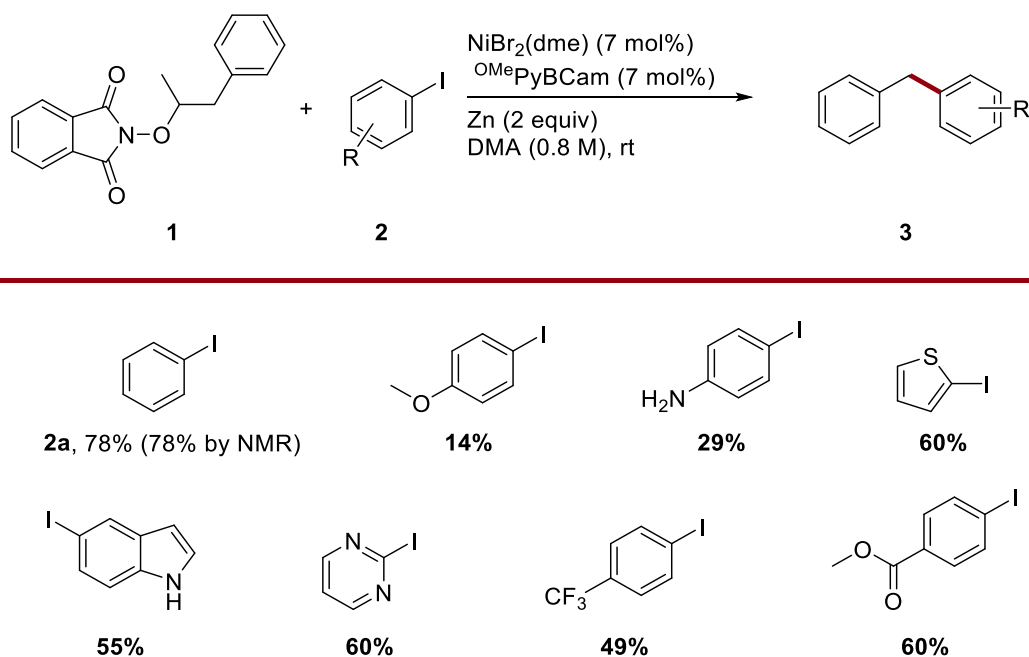
^a Reactions were run on a 0.80 mmol scale in 1 mL of solvent for 24 h. ^b GC yield vs internal standard (dodecane), NMR yields in parenthesis.

Figure 3.6 Product Distribution at Various Substrate Ratios

Reactions were run on a 0.80 mmol scale in 1 mL of solvent for 24 h. GC yield vs internal standard (dodecane).

3.3.7. Potential Substrates

Due to the apparent necessity of a benzylic radical to be formed for productive chemistry to occur, the process of discovering other reactive NAP ethers for productive cross-coupling has been a challenge. Indeed, in the seminal work from the Chen group where NAP ethers are used to generate alkyl equivalents, there is an overwhelming representative of benzylic radical-forming substrates used. These types of molecules may be easily coupled under our current conditions (Figure 3.9). Despite this impediment, a screen surveying some potential aryl iodide coupling partners of representative functionalities showed that the conditions prove general for the oxidative addition portion of the reaction (Figure 3.10). As long as suitable NAP ethers can be identified, the overall general reaction methodology bodes well.

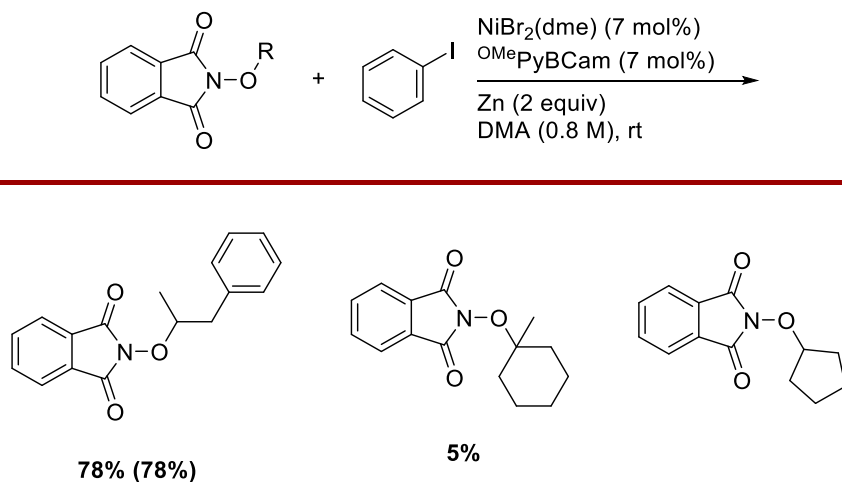
Figure 3.7 Potentially Suitable N-Alkoxyphthalimide Ether Substrates**Figure 3.8** Initial Aryl Iodide Survey

Reactions were run on a 0.80 mmol scale in 1 mL of solvent for 24 h. GC yield vs internal standard (dodecane).

Another potential avenue for this chemistry would be the utilization of ring-opening NAP ethers, which would afford terminal aldehydes in the coupling with aryl iodides, as the ring opening forms an intermediate carbon centered radical on the opposite end of the alkyl chain,

disfavoring the β -scission and allowing for aldehydic functionality to persist. These sorts of NAP ethers have thus far only given trace amounts of product under the optimized conditions (Figure 3.11), but these results are promising given that the benchmark reaction for this chemistry also afforded product in only trace amounts. Though we have tried the cyclohexanol and cyclopentanol-derived ethers for this chemistry, the Chen group reports their best yields with a cyclopropanol-derived NAP ether, so it could be possible that the added ring strain of such a system would work in our favor for radical formation and subsequent cross-coupling.

Figure 3.9 Potential Ring-opening Substrates Under Current Reaction Conditions

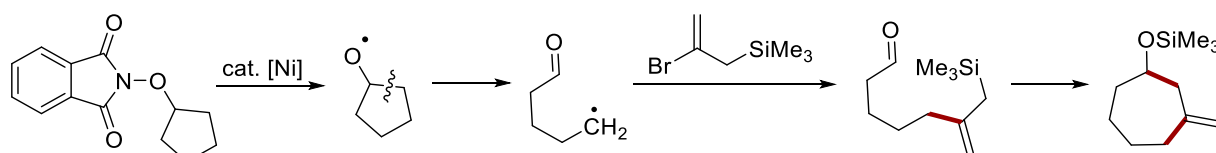


^a Reactions were run on a 0.80 mmol scale in 1 mL of solvent for 24 h. ^b GC yield vs internal standard (dodecane), NMR yields in parenthesis.

One last option to expand upon the substrate scope that is in the process of being investigated is the potential use of cyclic NAP ethers for ring-expansion chemistry when coupled with bromoallyl silanes (Figure 3.12). This idea was inspired by the Trost group's bifunctional annulation reagents¹⁰⁰, and the addition of such a radical acceptor would lead to a net two-carbon ring expansion of the cycloalkanol-derived NAP ether. Given that work in the Reisman group

shows that allylsilanes are tolerated under similar cross-coupling conditions to those that we have optimized¹⁰¹, this could allow for a new method to synthesize 7- or 8-membered ring systems from alcohols.

Figure 3.10 Potential Ring-expansion with NAP Ether and Bromoallyl Silanes



3.4. Conclusion

The development of a nickel-catalyzed cross-electrophile coupling reaction between aryl halides NAP ethers based upon analogous chemistry found with NHP esters has allowed and will continue to allow for development of wider substrate availability for the formation of C(sp²)-C(sp³) bonds. We have proven that Ni alone is capable of activating NAP ethers via a single electron transfer, allowing this methodology to occur without the need of visible light catalysis. The NAP ester can then generate an alkoxy radical, which can undergo β -scission prior to subsequent capture of the transient alkyl radical formed by a Ni(II)aryl to then reductively eliminate, forming a C(sp²)-C(sp³) bond. This new reaction is made possible by the discovery of the PyBCam ligand class. These new methods also allow for access to functionalities inherently native to carboxylic acids and alcohols, since NHP esters and NAP ethers can be readily synthesized from each of these functionalities, respectively. Both starting materials also offer increased stability over the analogous alkyl nucleophile or halide, as both redox active moieties are bench stable, generally crystalline, and thermally stable. Hopefully, the continued investigation of reagents that deliver

alkyl radical equivalents derived from commodity functional groups to cross-coupling reactions will expand the toolkit of the synthetic chemistry community exponentially.

3.5. Experimental

3.5.1. Materials

Zinc flake (-325 mesh) was purchased from Alfa Aesar, stored in a nitrogen filled glovebox, and used as received. Nickel(II) bromide ethylene glycol dimethyl ether ($\text{NiBr}_2(\text{dme})$) was synthesized according to the literature procedure and stored in a nitrogen filled glovebox.¹⁰² The amount of dme present in the $\text{NiBr}_2(\text{dme})$ was determined by elemental analysis and the mass of $\text{NiBr}_2(\text{dme})$ was calculated accordingly. $\text{Ni}(\text{cod})_2$ was purchased from Strem Chemicals and used soon after receiving as this material decomposes over time.

Pyridine-2,6-bis(carboximidamide)•2HCl (PyBCam•2HCl) was synthesized according to the literature procedure.¹⁰³ Pyridine-2,6-bis(N-cyanocarboximidine) (PyBCamCN) was synthesized according the literature procedure.¹⁰⁴ All other ligands tested were purchased from commercial suppliers and used as received.

Dry DMA (N,N-Dimethylacetamide, anhydrous, 99.8%) was purchased from Sigma Aldrich and used without purification.

3.5.2. General Methods

^1H nuclear magnetic resonance (NMR) spectroscopy chemical shifts are reported in ppm and referenced to TMS (tetramethylsilane) in CDCl_3 ($\delta = 0$ ppm) or the residual solvent peak for CDCl_3 ($\delta = 7.26$ ppm). For ^{13}C NMR and ^{19}F NMR chemical shifts, the residual solvent peak (CDCl_3 , $\delta = 77.00$ ppm) and TMS ($\delta = 0$ ppm) were used as references. Chemical shifts are reported

in parts per million (ppm), multiplicities are indicated by s (singlet), d (doublet), t (triplet), q (quartet), m (multiplet) and br (broad). Coupling constants (J) are reported in Hertz.

GC analyses were performed on an Agilent 7890A GC equipped with dual DB-5 columns (20 m \times 180 μ m \times 0.18 μ m), dual FID detectors, and hydrogen as the carrier gas. A sample volume of 1 μ L was injected at a temperature of 300 $^{\circ}$ C and a 100:1 split ratio. The initial inlet pressure was 20.3 psi but varied as the column flow was held constant at 1.8 mL/min for the duration of the run. The initial oven temperature of 50 $^{\circ}$ C was held for 0.46 min followed by a temperature ramp of 65 $^{\circ}$ C/min up to 300 $^{\circ}$ C. The temperature was held at 300 $^{\circ}$ C for 3 min. The total run time was \sim 7.3 min and the FID temperature was 325 $^{\circ}$ C.

Chromatography was performed on silica gel (EMD, silica gel 60, particle size 0.040-0.063 mm) using standard flash techniques or on 40 g HP Silica column (catalog 69-2203-347) using a Teledyne Isco Rf- 200 (detection at 210 nm and 340 nm). Products were visualized by UV-vis.

Elemental analyses were performed by CENTC Elemental Analysis Facility at University of Rochester, funded by NSF CHE-0650456.

GCMS was done with a Shimadzu GCMS-2010S. For non-volatile compounds, high resolution mass spectra (HRMS) mass spectrometry data was collected on a Thermo Q ExactiveTM Plus (ESI-Q-IT-MS) (thermofisher.com) via flow injection with electrospray ionization. An ASAP-MSTM source (ionSence, Saugus, MA) on the Thermo Q ExactiveTM Plus was used to obtain HRMS for volatile compounds analyzed by GCMS. This HRMS data was acquired by the chemistry mass spectrometry facility at the University of Wisconsin- Madison.

3.5.3. General Reaction Procedures

3.5.3.1. Synthesis of *N*-Alkoxyphthalimide Ethers⁹¹

To a solution of the corresponding alcohol (5.0 mmol), PPh₃ (1.57 g, 6.0 mmol), and *N*-hydroxyphthalimide (6.0 mmol) in THF (10 mL) was added diisopropyl azodicarboxylate (1.2 mL, 6.0 mmol) over 10 min at rt. The resulting mixture was then stirred for 24 h, taken up in EtOAc (20 mL), and washed with saturated NaHCO₃ (3 × 20 mL) and brine (2 × 30 mL). The organic layers were dried over anhydrous Na₂SO₄, concentrated in vacuo, and subjected to flash chromatography to afford the desired *N*-alkoxyphthalimide derivatives. The product can also be purified by recrystallization with EtOH in some cases.

3.5.3.2. General Procedure for the Synthesis of (dtbbpy)Ni^{II}(Ar)(Br)¹⁰⁵

In a nitrogen-filled glove box, a 20 mL-scintillation vial equipped with a PTFE-coated stir bar was charged with Ni(cod)₂ (275 mg, 1.0 mmol), 4,4'-di-*tert*-butyl-2,2'-bipyridine (268 mg, 1.0 mmol) and anhydrous THF (3 mL). The resulting deep purple solution was left to stir for 2 hours at rt. Aryl halide (1.1 mmol up to 103 mmol depending upon reactivity) was added and the reaction vial was left to stir for 20 min at rt. The resulting dark red solution was precipitated via addition of pentane (10 mL). The precipitate was collected on a frit (disposable, 18 mL, 10 micron polyethylene), rinsed with pentane and residual solvent was removed under vacuum to give the corresponding (dtbbpy)Ni^{II}(Ar)(X) complex.

3.5.3.3. Procedure for Study of *N*-Alkoxyphthalimide Ether Activation

In a nitrogen-filled glovebox, a 1-dram vial was equipped with a PTFE-coated stir bar was added 2-((1-phenylpropan-2-yl)oxy)isoindoline-1,3-dione (29.7 mg, 0.1 mmol), Hantzsch ester (126.7 mg, 0.5 mmol), 10 μ L of dodecane (internal standard) and 1 mL of the corresponding solvent (DMA or MeOH). The dram vial was fitted with a septa cap and removed from the glovebox. Reactions were allowed to stir at 1250 rpm at rt on a blue LED light setup or at 100 °C in ambient light without Hantzsch ester. After 1 h, a 25 μ L aliquot of the reaction mixture was removed with a 50 μ L gas-tight syringe. The aliquot was diluted with diethyl ether (1.5 mL), quenched with 50 μ L of 1 M aqueous NaHSO₄, and filtered through a short silica plug (1.5 cm) in a pipette packed with glass wool. The filtrate was analyzed by gas chromatography and percent yield was calculated versus dodecane as an internal standard.

3.5.3.4. Stoichiometric Reaction Between Ni Species and *N*-Alkoxyphthalimide Ethers

In a nitrogen-filled glovebox, a 1-dram vial was equipped with a PTFE-coated stir bar was added (bpy)Ni^{II}(*o*-tolyl)Br (0.0125 mmol), Hantzsch ester (160 mg, 0.63 mmol), 2-((1-Phenylpropan-2-yl)oxy)isoindoline-1,3-dione (37 mg, 0.125 mmol), 10 μ L of dodecane (internal standard) and 1 mL of DMA. The dram vial was fitted with a septa cap and removed from the glovebox and placed on a blue LED light setup, where it was allowed to stir at 1250 rpm. After 1 h, a 25 μ L aliquot of the reaction mixture was removed with a 50 μ L gas-tight syringe. The aliquot was diluted with diethyl ether (1.5 mL), quenched with 50 μ L of 1 M aqueous NaHSO₄, and filtered through a short silica plug (1.5 cm) in a pipette packed with glass wool. The filtrate was

analyzed by gas chromatography and percent yield was calculated versus dodecane as an internal standard.

3.5.3.5. General Procedure for the Ni-Catalyzed Coupling of Aryl Iodides and *N*-Alkoxyphthalimide Ethers

In a nitrogen-filled glovebox, a 1-dram vial was equipped with a PTFE-coated stir bar was added NiBr₂(dme) (17 mg, 7 mol%, 0.056 mmol), ^{OMe}PyBCam (15 mg, 7 mol%, 0.056 mmol), Hantsch ester (914 mg, 4.5 equiv, 3.6 mmol), 2-((1-phenylpropan-2-yl)oxy)isoindoline-1,3-dione (337.6 mg, 1.5 equiv, 1.2 mmol), zinc (105.6 mg, 2.0 equiv, 1.6 mmol), iodobenzene (89.2 μ L, 1 equiv, 0.8 mmol), 10 μ L of dodecane (internal standard) and 1 mL of DMA. The dram vial was fitted with a septa cap and removed from the glovebox and placed on a blue LED light setup, where it was allowed to stir at 1250 rpm. After 18–48 h, a 25 μ L aliquot of the reaction mixture was removed with a 50 μ L gas-tight syringe. The aliquot was diluted with diethyl ether (1.5 mL), quenched with 50 μ L of 1 M aqueous NaHSO₄, and filtered through a short silica plug (1.5 cm) in a pipette packed with glass wool. The filtrate was analyzed by gas chromatography and percent yield was calculated versus dodecane as an internal standard.

3.5.3.6. Current Best General Procedure for the Ni-Catalyzed Coupling of Aryl Iodides and *N*-Alkoxyphthalimide Ethers

In a nitrogen-filled glovebox, a 1-dram vial was equipped with a PTFE-coated stir bar was added NiBr₂(dme) (17 mg, 7 mol%, 0.056 mmol), ^{OMe}PyBCam (15 mg, 7 mol%, 0.056 mmol), 2-((1-phenylpropan-2-yl)oxy)isoindoline-1,3-dione (337.6 mg, 1.5 equiv, 1.2 mmol), zinc (105.6 mg, 2.0 equiv, 1.6 mmol), iodobenzene (89.2 μ L, 1 equiv, 0.8 mmol), 10 μ L of dodecane (internal

standard) and 1 mL of DMA. The dram vial was fitted with a septa cap and removed from the glovebox allowed to stir at 1250 rpm at rt. After 18–48 h, a 25 μ L aliquot of the reaction mixture was removed with a 50 μ L gas-tight syringe. The aliquot was diluted with diethyl ether (1.5 mL), quenched with 50 μ L of 1 M aqueous NaHSO₄, and filtered through a short silica plug (1.5 cm) in a pipette packed with glass wool. The filtrate was analyzed by gas chromatography and percent yield was calculated versus dodecane as an internal standard.

3.5.4. Product Characterization

2-((1-Phenylpropan-2-yl)oxy)isoindoline-1,3-dione⁹¹ General condition from 1-phenyl-2-propanol (5.00 g): 96% yield (9.9 g). White solid. ¹H NMR (500 MHz, CDCl₃) δ 7.82 (dd, J = 5.4, 3.1 Hz, 2H), 7.74 (dd, J = 5.5, 3.1 Hz, 2H), 7.28 – 7.25 (m, 4H), 7.21 – 7.17 (m, 1H), 4.68 (dt, J = 7.9, 6.0 Hz, 1H), 3.24 (dd, J = 13.8, 5.6 Hz, 1H), 2.89 (dd, J = 13.8, 7.8 Hz, 1H), 1.33 (d, J = 6.2 Hz, 3H). ¹³C{¹H} NMR (126 MHz, CDCl₃) δ 164.27, 137.13, 134.43, 129.30, 128.96, 128.43, 126.49, 123.48, 84.70, 41.38, 18.33. Our characterization data are consistent with those previously reported.

Acetolucosyl-phthalimide ether General condition from acetoglycosyl bromide (2.00 g): 42% yield (1.0 g). White solid. ¹H NMR (500 MHz, CDCl₃) δ 7.89 (dd, J = 5.5, 3.1 Hz, 2H), 7.80 (dd, J = 5.5, 3.1 Hz, 2H), 5.34 – 5.32 (m, 2H), 5.29 – 5.24 (m, 1H), 5.15 – 5.12 (m, 1H), 4.36 (dd, J = 12.3, 4.9 Hz, 1H), 4.17 (dd, J = 12.4, 2.8 Hz, 1H), 3.79 (ddd, J = 9.9, 4.9, 2.7 Hz, 1H), 2.22 (s, 3H), 2.08 (s, 3H), 2.07 (s, 3H), 2.05 (s, 3H). ¹³C{¹H} NMR (126 MHz, CDCl₃) δ 170.60, 170.13,

169.51, 169.28, 162.61, 134.79, 128.76, 123.85, 105.14, 72.46, 72.39, 69.63, 68.17, 61.80, 20.70, 20.69, 20.62, 20.57.

(dtbbpy)Ni^{II}(*o*-tolyl)Br¹⁰⁵ General condition for nickel complex synthesis: 55% yield (276 mg).

Red solid. ¹H NMR (500 MHz, CD₂Cl₂) δ 9.25 (d, J = 5.9 Hz, 1H), 7.86 (d, J = 1.9 Hz, 1H), 7.81 (d, J = 2.1 Hz, 1H), 7.53 (dd, J = 7.1, 1.4 Hz, 1H), 7.51 (dd, J = 5.9, 2.0 Hz, 1H), 7.12 (dd, J = 6.3, 2.1 Hz, 1H), 7.03 (d, J = 6.2 Hz, 1H), 6.84 – 6.72 (m, 3H), 3.03 (s, 3H), 1.41 (s, 10H), 1.34 (s, 9H). ¹³C{¹H} NMR (126 MHz, CD₂Cl₂) δ 150.58, 150.44, 136.08, 127.24, 123.65, 123.40, 122.98, 122.31, 117.53, 116.86, 53.93, 53.72, 53.50, 53.28, 53.07, 30.07, 29.86. Our characterization data is consistent with those previously reported.

References

- (1) Campeau, L. -C.; Hazari, N. Cross-Coupling and Related Reactions: Connecting Past Success to the Development of New Reactions for the Future. *Organometallics* 2019, 38, 1, 3–35.
- (2) Nicolaou, K. C.; Bulger, P. G.; Sarlah, D. Palladium-Catalyzed Cross-Coupling Reactions in Total Synthesis. *Angew. Chem., Int. Ed.* 2005, 44, 4442–4489.
- (3) Corbet, J.-P.; Mignani, G. Selected Patented Cross-Coupling Reaction Technologies. *Chem. Rev.* 2006, 106, 2651–2710.
- (4) Magano, J.; Dunetz, J. R. Large-Scale Applications of Transition Metal-Catalyzed Couplings for the Synthesis of Pharmaceuticals. *Chem. Rev.* 2011, 111, 2177–2250.
- (5) Buchwald, S. L. Cross Coupling. *Acc. Chem. Res.* 2008, 41, 1439-1439.
- (6) *New Trends in Cross-Coupling: Theory and Applications*; Colacot, T. J., Ed.; RSC Catalysis Series, No. 21; Royal Society of Chemistry: Cambridge, U.K., 2015.
- (7) Gildner, P. G.; Colacot, T. J. Reactions of the 21st Century: Two Decades of Innovative Catalyst Design for Palladium-Catalyzed Cross-Couplings. *Organometallics* 2015, 34, 5497–5508.
- (8) Ruiz-Castillo, P.; Buchwald, S. L. Applications of Palladium-Catalyzed C–N Cross-Coupling Reactions. *Chem. Rev.* 2016, 116, 12564–12649.
- (9) Hazari, N.; Melvin, P. R.; Mohadjer Beromi, M. Well-Defined Nickel and Palladium Precatalysts for Cross-Coupling. *Nat. Rev. Chem.* 2017, 1, 0025.
- (10) Goldfogel, M. J.; Huang, L.; Weix, D. J. Cross-Electrophile Coupling. In *Nickel Catalysis in Organic Synthesis*; Ogoshi, S., Ed.; Wiley-VCH: Weinheim, 2020; pp 183–222.
- (11) Wang, X.; Dai, Y.; Gong, H. Nickel-Catalyzed Reductive Couplings. *Top. Curr. Chem.* 2016, 374, 43.

- (12) Everson, D. A.; Weix, D. J. Cross-Electrophile Coupling: Principles of Reactivity and Selectivity. *J. Org. Chem.* 2014, 79, 4793–4798.
- (13) Knappke, C. E. I.; Grupe, S.; Gärtner, D.; Corpet, M.; Gosmini, C.; Jacobi von Wangelin, A. Reductive Cross-Coupling Reactions between Two Electrophiles. *Chem. - Eur. J.* 2014, 20, 6828–6842.
- (14) Frisch, A. C.; Beller, M. Catalysts for Cross-Coupling Reactions with Non-Activated Alkyl Halides. *Angew. Chem., Int. Ed.* 2005, 44, 674–688.
- (15) Rudolph, A.; Lautens, M. Secondary Alkyl Halides in Transition-Metal-Catalyzed Cross-Coupling Reactions. *Angew. Chem., Int. Ed.* 2009, 48, 2656–2670.
- (16) Jana, R.; Pathak, T. P.; Sigman, M. S. Advances in Transition Metal (Pd,Ni,Fe)-Catalyzed Cross-Coupling Reactions Using Alkyl-organometallics as Reaction Partners. *Chem. Rev.* 2011, 111, 1417–1492.
- (17) Manolikakes, G. 3.08 Coupling Reactions Between sp^3 and sp^2 Carbon Centers A2. In *Comprehensive Organic Synthesis II, 2nd ed.*; Knochel, P., Ed.; Elsevier: Amsterdam, 2014; pp 392–464.
- (18) While there is a total of about 2.3 million available organometallic or halide aryl reagents commercially available, there are only 480,000 alkyl sources, as these tend to be less stable. Source: eMolecules database, accessed 2019-04-28.
- (19) Given the numbers in citation (2) for alkyl sources, a great deal more chemistry could be accessed by adding OH and COOH derived alkyl equivalents, as there are almost 3 million commercially available alkyl sources in this reagent pool. Source: eMolecules database, accessed 2019-04-28.
- (20) Dieter, R. K. Reaction of Acyl Chlorides with Organometallic Reagents: A Banquet Table of Metals for Ketone Synthesis. *Tetrahedron* 1999, 55, 4177–4236.
- (21) O'Brien, E. M.; Bercot, E. A.; Rovis, T. Decarbonylative Cross-Coupling of Cyclic Anhydrides: Introducing Stereochemistry at an sp^3 Carbon in the Cross-Coupling Event. *J. Am. Chem. Soc.* 2003, 125, 10498–10499.

- (22) Muto, K.; Yamaguchi, J.; Musaev, D. G.; Itami, K. Decarbonylative Organoboron Cross-Coupling of Esters by Nickel Catalysis. *Nat. Commun.* 2015, 6, 7508-7516.
- (23) Miyaura, N.; Yamada, K.; Suzuki, A. A new Stereospecific Cross-Coupling by the Palladium-Catalyzed Reaction of 1-Alkenylboranes with 1-Alkenyl or 1-Alkynyl Halides. *Tetrahedron Lett.* 1979, 20, 3437-3440.
- (24) Kolbe, H. Chrysammensäure. *Ann. Chem. Pharm.* 1848, 64, 339.
- (25) Borodin, A. Ueber Bromvaleriansäure und Brombuttersäure. *Ann. Chem. Pharm.* 1861, 119, 121.
- (26) Hunsdiecker, H.; Hunsdiecker, C. Über den Abbau der Salze aliphatischer Säuren durch Brom. *Ber. Dtsch. Chem. Ges. B* 1942, 75, 291.
- (27) Hofmann, A. W. Zur Kenntniss des Piperidins und Pyridins. *Ber. Dtsch. Chem. Ges.* 1879, 12, 984.
- (28) Hofmann, A. W. Zur Kenntniss der Coniin-Gruppe. *Ber. Dtsch. Chem. Ges.* 1885, 18, 5.
- (29) Löffler, K.; Freytag, C. Über eine neue Bildungsweise von N-alkylierten Pyrrolidinen. *Ber. Dtsch. Chem. Ges.* 1909, 42, 3427.
- (30) Wolff, M. E. Cyclization of N-Halogenated Amines (The Hofmann-Löffler Reaction). *Chem. Rev.* 1963, 63, 55.
- (31) McMurry, J. E.; Fleming, M. P. New method for the reductive coupling of carbonyls to olefins. Synthesis of beta-carotene. *J. Am. Chem. Soc.* 1974, 96, 4708.
- (32) McMurry, J. E. Carbonyl-coupling reactions using low-valent titanium. *Chem. Rev.* 1989, 89, 1513.
- (33) Namy, J. L.; Girard, P.; Kagan, H. *Nouv. J. Chim.* 1977, 1, 5.

- (34) Girard, P.; Namy, J. L.; Kagan, H. B. Divalent lanthanide derivatives in organic synthesis. 1. Mild preparation of samarium iodide and ytterbium iodide and their use as reducing or coupling agents. *J. Am. Chem. Soc.* 1980, *102*, 2693.
- (35) Kagan, H. B. Twenty-five years of organic chemistry with diiodosamarium: An overview. *Tetrahedron* 2003, *59*, 10351.
- (36) Gomberg, M. An instance of trivalent carbon: Triphenylmethyl. *J. Am. Chem. Soc.* 1900, *22*, 757.
- (37) Kharasch, M. S.; Mayo, F. R. The Peroxide Effect in the Addition of Reagents to Unsaturated Compounds. I. The Addition of Hydrogen Bromide to Allyl Bromide. *J. Am. Chem. Soc.* 1933, *55*, 2468.
- (38) Kharasch, M. S.; Engelmann, H.; Mayo, F. R. The Peroxide effect in the addition of reagents to unsaturated compounds. XV. The addition of hydrogen bromide to 1- and 2-bromo- and chloropropenes. *J. Org. Chem.* 1937, *2*, 288.
- (39) Kharasch, M. S.; Jensen, E. V.; Urry, W. H. Addition of carbon tetrachloride and chloroform to olefins. *Science* 1945, *102*, 128.
- (40) Bachmann, W. E.; Wiselogle, F. Y. The Relative Stability of Pentaarylethanes. III. The Reversible Dissociation of Pentaarylethanes. *J. Org. Chem.* 1936, *1*, 354.
- (41) Hey, D. H.; Perkins, M. J.; William, G. H. Mechanisms of free-radical aromatic substitution. *Tetrahedron Lett.* 1963, *4*, 445.
- (42) Fischer, H. Unusual selectivities of radical reactions by internal suppression of fast modes. *J. Am. Chem. Soc.* 1986, *108*, 3925.
- (43) Daikh, B. E.; Finke, R. G. The persistent radical effect: a prototype example of extreme, 105 to 1, product selectivity in a free-radical reaction involving persistent $\cdot\text{CoII}$ [macrocycle] and alkyl free radicals. *J. Am. Chem. Soc.* 1992, *114*, 2938.
- (44) Arends, I. W. C. E.; Ingold, K. U.; Wayner, D. D. M. A Mechanistic Probe for Oxygen Activation by Metal Complexes and Hydroperoxides and Its Application to Alkane

- Functionalization by $[\text{FeIII}(\text{Cl}_2\text{tris}(2\text{-pyridinylmethyl)amine})]^+ \text{BF}_4^-$. *J. Am. Chem. Soc.* 1995, *117*, 4710.
- (45) Fischer, H. The Persistent Radical Effect: A Principle for Selective Radical Reactions and Living Radical Polymerizations. *Chem. Rev.* 2001, *101*, 3581.
- (46) Studer, A. The Persistent Radical Effect in Organic Synthesis. *Chem. - Eur. J.* 2001, *7*, 1159.
- (47) Griller, D.; Ingold, K. U. Persistent carbon-centered radicals. *Acc. Chem. Res.* 1976, *9*, 13.
- (48) Bush, J. B., Jr.; Finkbeiner, H. Oxidation reactions of manganese(III) acetate. II. Formation of γ -lactones from olefins and acetic acid. *J. Am. Chem. Soc.* 1968, *90*, 5903.
- (49) Heiba, E. I.; Dessau, R. M.; Koehl, W. J., Jr. Oxidation by metal salts. I. Reaction of lead tetraacetate with toluene. *J. Am. Chem. Soc.* 1968, *90*, 5905.
- (50) Corey, E. J.; Kang, M. C. A new and general synthesis of polycyclic γ -lactones by double annulation. *J. Am. Chem. Soc.* 1984, *106*, 5384.
- (51) Snider, B. B.; Mohan, R.; Kates, S. A. Manganese(III)-based oxidative free-radical cyclization. Synthesis of (\pm)-podocarpic acid. *J. Org. Chem.* 1985, *50*, 3659.
- (52) Pettus, T. R. R.; Chen, X.-T.; Danishefsky, S. J. A Fully Synthetic Route to the Neurotrophic Illicinones by Sequential Aromatic Claisen Rearrangements. *J. Am. Chem. Soc.* 1998, *120*, 12684.
- (53) Bell, F. A.; Ledwith, A.; Sherrington, D. C. Cation-radicals: tris-(*p*-bromophenyl)amminium perchlorate and hexachloroantimonate. *J. Chem. Soc. C* 1969, *20*, 2719.
- (54) Ledwith, A. Cation radicals in electron transfer reactions. *Acc. Chem. Res.* 1972, *5*, 133.
- (55) Minisci, F.; Bernardi, R.; Bertini, F.; Galli, R.; Perchinummo, M. Nucleophilic character of alkyl radicals—VI: A new convenient selective alkylation of heteroaromatic bases. *Tetrahedron* 1971, *27*, 3575.

- (56) Minisci, F.; Vismara, E.; Fontana, F.; Morini, G.; Serravalle, M.; Giordano, C. Polar effects in free-radical reactions. Rate constants in phenylation and new methods of selective alkylation of heteroaromatic bases. *J. Org. Chem.* 1986, *51*, 4411.
- (57) Citterio, A.; Minisci, F.; Porta, O.; Sesana, G. Nucleophilic character of the alkyl radicals. 16. Absolute rate constants and the reactivity-selectivity relationship in the homolytic aromatic alkylation. *J. Am. Chem. Soc.* 1977, *99*, 7960.
- (58) Kochi, J. K. Electron-transfer mechanisms for organometallic intermediates in catalytic reactions. *Acc. Chem. Res.* 1974, *7*, 351.
- (59) Studer, A.; Curran, D. P. Catalysis of Radical Reactions: A Radical Chemistry Perspective. *Angew. Chem., Int. Ed.* 2016, *55*, 58.
- (60) Renneke, R. F.; Hill, C. L. Homogeneous catalytic photochemical functionalization of alkanes by polyoxometalates. *J. Am. Chem. Soc.* 1986, *108*, 3528.
- (61) Pandey, G. Photoinduced electron transfer (PET) in organic synthesis. *Top. Curr. Chem.* 1993, *168*, 176.
- (62) Delduc, P.; Tailhan, C.; Zard, S. Z. A convenient source of alkyl and acyl radicals. *J. Chem. Soc., Chem. Commun.* 1988, *4*, 308.
- (63) Destarac, M.; Charmot, D.; Franck, X.; Zard, S. Z. Dithiocarbamates as universal reversible addition-fragmentation chain transfer agents. *Macromol. Rapid Commun.* 2000, *21*, 1035.
- (64) Zard, S. Z. *In Radicals in Organic Synthesis*; Renaud, P., Sibi, M. P., Eds.; Wiley: New York, 2008; Vol. 1, p 90.
- (65) Zard, S. Z. On the Trail of Xanthates: Some New Chemistry from an Old Functional Group. *Angew. Chem., Int. Ed. Engl.* 1997, *36*, 672.
- (66) Quiclet-Sire, B.; Zard, S. Z. Some Aspects of the Radical Chemistry of Xanthates. *Chimia* 2012, *66*, 404.
- (67) Quiclet-Sire, B.; Zard, S. Z. Powerful Carbon-Carbon Bond Forming Reactions Based on a Novel Radical Exchange Process. *Chem. - Eur. J.* 2006, *12*, 6002.

- (68) Quiclet-Sire, B.; Zard, S. Z. Fun with radicals: Some new perspectives for organic synthesis. *Pure Appl. Chem.* 2010, 83, 519.
- (69) Okada, K.; Okamoto, K.; Oda, M. A New and Practical Method of Decarboxylation: Photosensitized Decarboxylation of *N*-Acyloxyphthalimides via Electron-Transfer Mechanism. *J. Am. Chem. Soc.* 1988, 110, 8736–8738.
- (70) Okada, K.; Okamoto, K.; Morita, N.; Okubo, K.; Oda, M. Photosensitized Decarboxylative Michael Addition Through *N*-(Acyloxy)phthalimides via an Electron-Transfer Mechanism. *J. Am. Chem. Soc.* 1991, 113, 9401–9402.
- (71) Nugent, W. A.; RajanBabu, T. V. Transition-metal-centered radicals in organic synthesis. Titanium(III)-induced cyclization of epoxy olefins. *J. Am. Chem. Soc.* 1988, 110, 8561.
- (72) RajanBabu, T. V.; Nugent, W. A. Intermolecular addition of epoxides to activated olefins: a new reaction. *J. Am. Chem. Soc.* 1989, 111, 4525.
- (73) RajanBabu, T. V.; Nugent, W. A. Selective Generation of Free Radicals from Epoxides Using a Transition-Metal Radical. A Powerful New Tool for Organic Synthesis. *J. Am. Chem. Soc.* 1994, 116, 986.
- (74) Mukaiyama, T.; Isayama, S.; Inoki, S.; Kato, K.; Yamada, T.; Takai, T. Oxidation-Reduction Hydration of Olefins with Molecular Oxygen and 2-Propanol Catalyzed by Bis(acetylacetonato)cobalt(II). *Chem. Lett.* 1989, 18, 449.
- (75) Kato, K.; Yamada, T.; Takai, T.; Inoki, S.; Isayama, S. Catalytic Oxidation–Reduction Hydration of Olefin with Molecular Oxygen in the Presence of Bis (1,3-diketonato) cobalt (II) Complexes. *Bull. Chem. Soc. Jpn.* 1990, 63, 179.
- (76) Zuo, Z.; Ahneman, D. T.; Chu, L.; Terrett, J. A.; Doyle, A. G.; MacMillan D. W. C. Merging Photoredox with Nickel Catalysis: Coupling of α -Carboxyl sp^3 -Carbons with Aryl Halides. *Science* 2014, 345, 6195, 437-440.
- (77) Noble, A.; McCarver, S. J.; MacMillan, D. W. C. Merging Photoredox and Nickel Catalysis: Decarboxylative Cross-Coupling of Carboxylic Acids with Vinyl Halides. *J. Am. Chem. Soc.* 2015, 137, 2, 624–627.

- (78) The coupling of a vinyl bromide with 3 equiv of cyclohexane carboxylic acid (78% yield) and 5-phenylvaleric acid (11% yield) were reported in ref 25.
- (79) Okada, K.; Okamoto, K.; Oda, M. Photochemical Chlorodecarboxylation via an Electron Transfer Mechanism. *J. Chem. Soc., Chem. Commun.* 1989, 1636–1637.
- (80) Okada, K.; Okubo, K.; Morita, N.; Oda, M. Reductive Decarboxylation of *N*-(Acyloxy)phthalimides via Redox-Initiated Radical Chain Mechanism. *Tetrahedron Lett.* 1992, 33, 7377–7380.
- (81) Okada, K.; Okubo, K.; Morita, N.; Oda, M. Redox-Mediated Decarboxylative Photo-Phenylselenenylation of *N*-Acyloxyphthalimides. *Chem. Lett.* 1993, 22, 2021–2024.
- (82) Schnermann, M. J.; Overman, L. E. A Concise Synthesis of (–)-Aplyviolene Facilitated by a Strategic Tertiary Radical Conjugate Addition. *Angew. Chem., Int. Ed.* 2012, 51, 9576–9580.
- (83) Pratsch, G.; Lackner, G. L.; Overman, L. E. Constructing Quaternary Carbons from *N*-(Acyloxy)phthalimide Precursors of Tertiary Radicals Using Visible-Light Photocatalysis. *J. Org. Chem.* 2015, 80, 6025–6036.
- (84) S. Biswas and D. J. Weix, Mechanism and Selectivity in Nickel-Catalyzed Cross-Electrophile Coupling of Aryl Halides with Alkyl Halides. *J. Am. Chem. Soc.* 2013, 135, 16192–16197.
- (85) Huihui, K. M. M.; Caputo, J. A.; Melchor, Z.; Olivares, A. M.; Spiewak, A. M.; Johnson, K. A.; DiBenedetto, T. A.; Kim, S.; Ackerman, L. K. G.; Weix, D. J., Decarboxylative Cross-Electrophile Coupling of *N*-Hydroxyphthalimide Esters with Aryl Iodides. *J. Am. Chem. Soc.* 2016, 138, 5016–5019.
- (86) König, W.; Geiger, R. A new method for synthesis of peptides: activation of the carboxyl group with dicyclohexylcarbodiimide using 1-hydroxybenzotriazoles as additives. *Chem. Ber.* 1969, 103, 788.
- (87) Carpino, L. A. 1-Hydroxy-7-azabenzotriazole. An efficient peptide coupling additive. *J. Am. Chem. Soc.* 1993, 115, 4397.

- (88) Cornella, J.; Edwards, J. T.; Qin, T.; Kawamura, S.; Wang, J.; Pan, C.-M.; Gianatassio, R.; Schmidt, M. A.; Eastgate, M. D.; Baran, P. S. Practical Ni-Catalyzed Aryl–Alkyl Cross-Coupling of Secondary Redox-Active Esters. *J. Am. Chem. Soc.* 2016, *138*, 2174–2177.
- (89) Kim, S.; Lee, T. A.; Song, Y., Facile Generation of Alkoxy Radicals from *N*-Alkoxyphthalimides. *Synlett* 1998, *1998*, 471-472.
- (90) Zlotorzynska, M.; Sammis, G. M., Photoinduced Electron-Transfer-Promoted Redox Fragmentation of *N*-Alkoxyphthalimides. *Org. Lett.* 2011, *13*, 6264-6267.
- (91) Zhang, J.; Li, Y.; Zhang, F.; Hu, C.; Chen, Y., Generation of Alkoxy Radicals by Photoredox Catalysis Enables Selective C(sp³)–H Functionalization under Mild Reaction Conditions. *Angew. Chem., Int. Ed.* 2016, *55*, 1872-1875.
- (92) Wang, C.; Harms, K.; Meggers, E., Catalytic Asymmetric Csp³-H Functionalization Under Photoredox Conditions by Radical Translocation and Stereocontrolled Alkene Addition. *Angew. Chem., Int. Ed.* 2016, *55*, 13495-13498.
- (93) Zhang, J.; Li, Y.; Xu, R.; Chen, Y., Donor-Acceptor Complex Enables Alkoxy Radical Generation for Metal-Free C(sp³)-C(sp³) Cleavage and Allylation/Alkenylation. *Angew. Chem., Int. Ed.* 2017, *56*, 12619-12623.
- (94) Shi, J.-L.; Wang, Z.; Zhang, R.; Wang, Y.; Wang, J., Visible-Light-Promoted Ring-Opening Alkynylation, Alkenylation, and Allylation of Cyclic Hemiacetals through β-Scission of Alkoxy Radicals. *Chem.–Eur. J.* 2019, *25*, 8992-8995.
- (95) Jia, K.; Chen, Y., Visible-Light-Induced Alkoxy Radical Generation for Inert Chemical Bond Cleavage/Functionalization. *Chem. Commun.* 2018, *54*, 6105-6112.
- (96) Capaldo, L.; Ravelli, D., Alkoxy Radicals Generation: Facile Photocatalytic Reduction of *N*-Alkoxyazinium or Azolium Salts. *Chem. Commun.* 2019, *55*, 3029-3032.
- (97) Kim, S.; Goldfogel, M. J.; Gilbert, M. M.; Weix, D. J., Nickel-Catalyzed Cross-Electrophile Coupling of Aryl Chlorides with Primary Alkyl Chlorides. *J. Am. Chem. Soc.* 2020, *142*, 9902-9907.

- (98) Hansen, E. C.; Li, C.; Yang, S.; Pedro, D.; Weix, D. J. Coupling of Challenging Heteroaryl Halides with Alkyl Halides via Nickel-Catalyzed Cross-Electrophile Coupling. *J. Org. Chem.* 2017, 82, 7085-7089.
- (99) Hughes, J. M. E.; Fier, P. S. Desulfonylative Arylation of Redox-Active Alkyl Sulfones with Aryl Bromides. *Org. Lett.* 2019, 21, 14, 5650–5654.
- (100) Trost, B. M.; Coppola, B. P., 2-Bromo-3-Trimethylsilylpropene. An Annulating Agent for Five-Membered Carbo- and Heterocycles. *J. Am. Chem. Soc.* 1982, 104, 6879-6881.
- (101) Hofstra, J. L.; Cherney, A. H.; Ordner, C. M.; Reisman, S. E., Synthesis of Enantioenriched Allylic Silanes via Nickel-Catalyzed Reductive Cross-Coupling. *J. Am. Chem. Soc.* 2018, 140, 139-142.
- (102) Lingamurthy, M.; Nalliboina, G. R.; Rao, M. V.; Rao, B. V.; Reddy, B. S.; Sampath Kumar, H. M. DDQ Mediated Stereoselective Intermolecular Benzylic CN Bond Formation: Synthesis of (–)-Cytoxazone, (–)-4-Epi-Cytoxazone and Their Analogues and Immunological Evaluation of Their Cytokine Modulating Activity. *Tetrahedron* 2017, 73, 1473–1481.
- (103) Pandey, G.; Laha, R.; Mondal, P. K. Heterocyclization Involving Benzylic C(Sp³)-H Functionalization Enabled by Visible Light Photoredox Catalysis. *Chem. Commun.* 2019, 55, 9689–9692.
- (104) Jouffroy, M.; Primer, D. N.; Molander, G. A. Base-Free Photoredox/Nickel Dual-Catalytic Cross-Coupling of Ammonium Alkylsilicates. *J. Am. Chem. Soc.* 2016, 138, 475–478.
- (105) Shields, B. J.; Kudisch, B.; Scholes, G. D.; Doyle, A. G. Long-Lived Charge-Transfer States of Nickel(II) Aryl Halide Complexes Facilitate Bimolecular Photoinduced Electron Transfer. *J. Am. Chem. Soc.* 2018, 140, 3035-3039.